
ACCO: Accumulate While You Communicate for Communication-Overlapped Sharded LLM Training

Adel Nabli^{1,2} Louis Fournier^{1*} Pierre Erbacher^{1*} Louis Serrano¹
Eugene Belilovsky² Edouard Oyallon¹

¹Sorbonne Université, CNRS, ISIR, Paris - France

²Mila - Quebec AI Institute, Concordia University, Montréal - Québec
edouard.oyallon@cnrs.fr

Abstract

Training LLMs relies on distributed implementations using multiple GPUs to compute gradients in parallel with sharded optimizers. However, synchronizing gradients in data parallel setups introduces communication overhead that grows with the number of workers, limiting parallelization efficiency. Local optimization algorithms reduce communications but incur high memory costs as they prevent optimizer state sharding, hindering scalability. To address this, we propose **AC**cumulate while **CO**mmunicate (ACCO), a memory-efficient optimization algorithm for distributed LLM training. By synchronizing delayed gradients while computing new ones, ACCO reduces GPU idle time and supports heterogeneous hardware. To mitigate the convergence issues caused by delayed updates, we introduce a novel technique ensuring training dynamics align with standard distributed optimization. Compared to ZeRO-1, our approach is significantly faster and scales effectively across heterogeneous hardware.

1 Introduction

Training Large Language Models (LLMs) with billions of parameters requires thousands of GPUs operating in parallel [71]. This process typically relies on distributed backpropagation [31] and gradient-based optimizers such as Adam [27] or AdamW [36]. However, distributed optimization at this scale is both memory- and communication-intensive. In standard data-parallel training, memory bottlenecks arise primarily from the optimizer’s internal states, especially under mixed-precision training. Techniques like ZeRO [55] mitigate this by sharding states across workers. Due to limited GPU memory and the large size of modern models, large-scale LLM training frameworks must rely on such sharded partitioning [64, 58, 2]. In addition to memory constraints, communication overhead becomes a dominant performance bottleneck, as synchronizing gradients and optimizer states across GPUs can exceed the time spent on actual computation [50], a problem expected to persist even with future hardware advances [53]. The impact of communication is further amplified by the cluster’s interconnect topology: effective sharding requires high-bandwidth links, and heterogeneous hardware or slow interconnects introduce straggler effects that slow down the entire system [15, 41].

To mitigate these issues, various communication-efficient distributed optimization algorithms have been proposed, particularly in settings with limited bandwidth such as Federated Learning. Local-update methods [66, 75, 40, 29, 14] reduce communication by splitting training into inner loops (local steps) and outer loops (synchronization steps). While this approach reduces frequency of communication, it introduces additional hyperparameters compared to standard training, scales poorly with the number of workers, and significantly increases memory requirements. For instance, the state-of-the-art CO2 method [69] requires memory overhead equivalent to four model copies—much more

*Equal contributions.

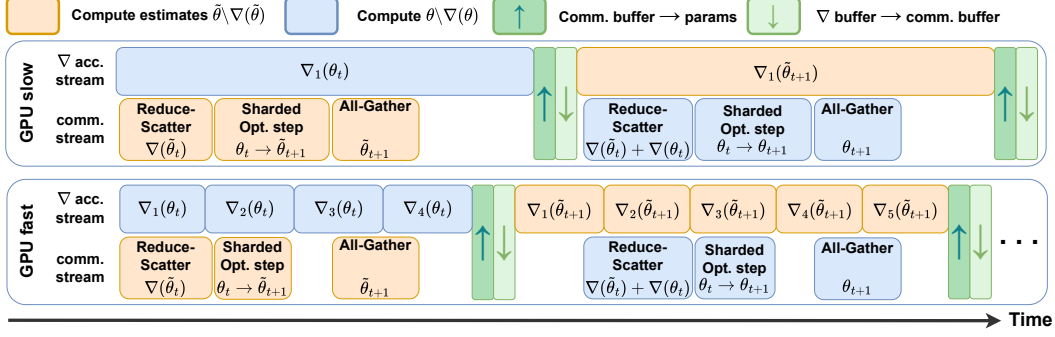


Figure 1: ACCO with a slow and a fast worker running in parallel, showing no idle time on both and hiding communications. The delayed update is compensated by splitting the mini-batch in two, leading to two steps in our timeline. The first uses half of the mini-batch to estimate "next step" parameters, and the second uses the full mini-batch to update them.

than standard distributed Adam and even further from its sharded variants [55]. Some local-update methods overlap communication with computation to hide latency, by executing both concurrently [74, 63, 82, 69]. However, this is challenging in sharded setups, since local updates typically require full optimizer states to be materialized, which defeats the purpose of memory or communication savings. A notable exception is ZeRO-Offload [60], which introduces the Delayed Parameter Update (DPU) mechanism: it runs gradient computation on GPUs while concurrently performing parameter updates on CPUs. Yet this approach suffers from one-step staleness—gradients [62] are applied to outdated parameters—which harms convergence [89]. Thus it struggles to match the performance or training dynamics of standard LLM training.

In this work, we introduce **AC**cumulate while you **CO**municate (ACCO), a new optimization method that unifies the benefits of communication–computation overlap with memory-efficient training, matching the training dynamics of AdamW DDP without new hyperparameters to tune. Specifically (1) ACCO allows overlapping gradient computation and parameter updates in the memory-efficient sharded optimizer settings. (2) It eliminates the need for outer loops, reducing memory and tuning overhead. (3) Crucially, it compensates for the one-step delay introduced by parallel execution of communication and computation by using a novel accumulation mechanism, which avoids the convergence degradation observed in DPU-style updates. (4) Unlike prior approaches, ACCO is compatible with sharded training frameworks and requires no warm-up phase. (5) In the case of SGD, we prove that ACCO achieves the standard convergence rate, and (6) we confirm it empirically: ACCO consistently preserves convergence quality across both homogeneous and heterogeneous environments, with training curves that *mirror* those of AdamW—just as our theory predicts. (7) Our experiments on diverse LLM pretraining and fine-tuning tasks show that ACCO delivers substantial wall-clock speedups and effective communication hiding compared to ZeRO—without compromising training stability or memory efficiency. The code to reproduce all our experiments is available at <https://github.com/edouardoyallon/acco>.

2 Related work

Local optimization methods for reducing communications. Local optimization methods perform several local model updates between periodic averaging. With the SGD optimizer, these algorithms predate the deep learning era [90, 39], and their convergence properties are still investigated nowadays [87, 66, 76, 42]. Due to their practical and efficient communication scheme, they have since been used for the Distributed Training of Deep Neural Networks (DNNs) with methods such as EASGD [82], SlowMo [75] or Post-local SGD [34, 50], and are ubiquitous in Federated Learning [40, 29, 32], broadening the choice of optimizers beyond SGD [59, 25, 10]. They have also recently been applied in LLM training [14, 7]. Overlapping communications over consecutive steps of local computations allows to hide communication bottlenecks, resulting in algorithms such as Overlap local-SGD [74], COCO-SGD [63], or CO2 [69]. Moreover, with heterogeneous hardware, they can adapt their local computation rate to their hardware capacity [13, 38]. Yet, this comes at the price of additional memory requirements: due to their local nature [11], not only do these

Table 1: Comparisons of characteristics and memory consumption. Ψ : number of parameters in the model. N : number of workers. K : memory multiplier of the optimizer (Adam or AdamW). For SlowMo [75] and CO2 [69], no mention of mixed precision training is made. We assume they use it and that their additional terms are stored in half precision. While no additional momentum is required for our method, we still need a negligible communication buffer compared to the optimizers’ states.

| Method | Overlap comm/comp | Hetero. hardware | No outer loop | Convergence Rates | Memory per replicas (K, N, Ψ)=(12, 64, 7.5B) |
|-------------|----------------------|---------------------|------------------|----------------------|--|
| DDP [31] | ✗ | ✗ | ✓ | ✓ | $(2+2+K)\Psi = 120$ GB |
| ZeRO-1 [55] | ✗ | ✗ | ✓ | ✓ | $(2+2+\frac{K}{N})\Psi = 31$ GB |
| ZeRO-2 [55] | ✗ | ✗ | ✓ | ✓ | $(2+\frac{2+K}{N})\Psi = 16$ GB |
| ZeRO-3 [55] | ✗ | ✗ | ✓ | ✓ | $(\frac{2+2+K}{N})\Psi = 2$ GB |
| SlowMo [75] | ~ | ✗ | ✗ | ~ | $(2+2+2\times 2+K)\Psi = 150$ GB |
| DiLoCo [14] | ✓ | ✗ | ✗ | ? | $(2+2+2\times 2+K)\Psi = 150$ GB |
| CO2 [69] | ✓ | ✗ | ✗ | ✓ | $(2+2+4\times 2+K)\Psi = 180$ GB |
| DPU [60] | ✓ | ✗ | ✓ | ✗ | $(2+2+2+\frac{K}{N})\Psi = 46$ GB |
| WP [8] | ✓ | ✗ | ✓ | ✗ | $(2+2+2+\frac{K}{N})\Psi = 46$ GB |
| ACCD (Ours) | ✓ | ✓ | ✓ | ✓ | $(2+2+2+\frac{K}{N})\Psi = 46$ GB |

methods prevent the use of sharded optimizers such as ZeRO [55], but they also introduce additional control variables [75, 42, 69], hindering their scalability as shown in Tab. 1. Moreover, catering for heterogeneous hardware is not straightforward, as using different numbers of local updates leads to models shifting at different speeds, requiring extra care to counter this effect [38]. On the contrary, ACCD does not lead to such disparities. Since all devices share the same parameters, the device speeds difference only affects the mini-batch size computation. Similarly, doing multiple local optimizer updates makes the approach incompatible with optimizer sharding.

Overlapping communications and computations. For the asynchronous approaches, some approaches overlap gradient and communication steps, either explicitly [5], or by modeling them with independent stochastic processes [45, 44, 17]. However, none of these works focus on memory efficiency. Thus, they introduce additional variables and do not consider sharding the optimizer states. Moreover, they do not study optimizers other than SGD, and extending their beneficial properties to adaptive methods commonly used for DNN training such as Adam is still an ongoing research topic [4]. Delays being intrinsic to distributed asynchronous optimization, there is a rich literature studying them. In the case of distributed SGD in a parameter server setting, while early analysis showed convergence rates depending on the *maximal* delay [1, 67], recent lines of work improved these dependencies [28, 77, 19], proving that asynchronous SGD beats standard mini-batch SGD even with unbounded delays [41, 46]. However, they only study plain SGD, which is hardly used for DNN training. In this context, some work focused on the interplay between SGD with momentum and delays [43, 81], while delay compensation schemes such as re-scaling updates [86, 78] or buffering them [49] were proposed for Federated Learning. But still, they only study versions of SGD and not adaptive methods commonly used for LLMs training such as Adam [27] or AdamW [36]. Closer to our work, DPU was introduced as a memory-efficient way to train LLMs by running the optimizer on the CPU while gradients are computed on the GPU [60, 33], inducing a one-step delay between the gradients computed and the corresponding optimizer step. To mitigate it, they advise starting training by warming up for several steps with standard DDP. Perhaps surprisingly, we find in our experiments that this one-step delay has a noticeable influence on the convergence of LLMs training, even when using warmup steps. Contrary to DPU, we remove the need for them, with no impact on the convergence of our training. Moreover, as it is not its purpose, DPU still runs communications in the gradient computation stream, and is thus impacted both by the communication overhead of scaling and hardware heterogeneity. Finally, in pipeline parallelism, gradient delays also affect computation, and weight prediction methods have been proposed to mitigate their effect [8, 79, 30, 80].

Memory-efficient distributed training of LLMs. The activation memory overhead required for training Transformers [72] can be mitigated for an extra computational cost by reconstructing the input with reversible architectures [62, 23, 37], or recomputing the activations via checkpointing [9]. Efficient LLM training also combines parallelism methods. Classical data parallelism (DP) [12]

suffers both from a high communication volume and a linear increase in memory due to the model replicas. ZeRO-DP [56] and Fully-Sharded DP [85] avoid this issue by sharding the model states (i.e., the optimizer states, gradients, and parameters) between workers. This comes at the cost of further increasing the synchronization between workers and the communication volume, which can be mitigated by compression [73], memory trade-offs [83], or delayed gradients [88]. The memory can be even more reduced using expensive CPU-GPU communications to unload states on the CPU [60, 57]. On the other hand, model parallelism partitions the DNN components for parallelization, either with tensor parallelism [64] by slicing a layer’s computation on several workers, or with pipeline parallelism, which divides a model into sets of layers trained in parallel on mini-batch slices. Popularized by [22], this method leaves some workers idling and an inefficient memory overhead [18]. Allowing delay in the gradients avoids worker idleness [47, 88] but exacerbates the memory overhead, which can be partially mitigated with gradient accumulation [48, 89] and activation checkpointing [26, 35]. Combining these frameworks results in the effective 3D parallelism [65].

3 Method

3.1 Background and Notations

We now present our framework as well as relevant prior methods for overlapping communication and computation from the perspective of an individual worker $i \in \{1, \dots, N\}$. The goal is to minimize a differentiable objective function $f : \mathbb{R}^d \rightarrow \mathbb{R}$. All workers are initialized with identical parameters $\theta^{(0)} \in \mathbb{R}^d$, and at each iteration t , worker i has access to a stochastic function $F : \mathbb{R}^d \times \Xi \rightarrow \mathbb{R}$, where Ξ is a sample space derived from its local data shard. The gradient estimates are assumed to be unbiased: $\mathbb{E}[\nabla F(\theta, \xi)] = \nabla f(\theta)$ for $\xi \sim \Xi$. This setup allows for flexible, even time-varying, batch sizes depending on each machine’s speed. However, for simplicity, we assume each worker computes a fixed-size minibatch of N_i samples per iteration. The resulting local gradient estimate is given by

$$\nabla F_i(\theta, \xi) \triangleq \frac{1}{N_i} \sum_{k=1}^{N_i} \nabla F(\theta, \xi_k), \quad \text{where } \xi = (\xi_1, \dots, \xi_{N_i}).$$

We also consider a generic optimizer, such as Adam or AdamW (common in LLM training), denoted by `Opt`. Applying the optimizer may require synchronizing internal states (e.g., moments, learning rates) across workers, which introduces a communication barrier. This synchronization can be particularly costly in settings involving optimizer sharding, and may substantially limit GPU throughput.

Distributed Data Parallelism (DDP). In a DDP setting, gradient computation and optimization steps are performed sequentially as follows, for a sequence of $\{\xi^{(t)}\}_t$:

$$g_i^{(t)} = \nabla F_i(\theta^{(t)}, \xi^{(t)}), \quad \theta^{(t+1)} = \text{Opt} \left(\theta^{(t)}, \sum_{i=1}^N \frac{N_i}{\sum_i N_i} g_i^{(t)} \right), \quad (\text{DDP})$$

where gradients are averaged across all N workers. As illustrated in this formulation, each step is fully synchronous and must follow a strict order, which limits the potential for overlapping communication and computation. A common strategy to address this limitation is to introduce two parameter buffers, denoted θ and $\tilde{\theta}$, where one is used for computation and the other for communication. Building on this insight, we next describe the main techniques used to achieve such overlap, and then ACCO.

Delayed Parameter Update (DPU). We describe the original DPU [60], and in our re-implementation, we run gradient communications in the same stream as the optimizer step, in parallel to the gradient computations. To prevent GPU from being idle at step t , gradients are accumulated over as many mini-batches as necessary until the communication process finishes. Then, DPU repeat the following, where each line can be run in parallel:

$$\begin{aligned} g_i^{(t+1)} &= \nabla F_i(\tilde{\theta}^{(t)}, \xi^{(t)}) \\ \tilde{\theta}^{(t+1)} &= \theta^{(t)}, \quad \theta^{(t+1)} = \text{Opt} \left(\theta^{(t)}, \sum_{i=1}^N \frac{N_i}{\sum_i N_i} g_i^{(t)} \right). \end{aligned} \quad (\text{DPU})$$

Remark that, except at the first step $t = 0$, the gradients used by `Opt` are computed on parameters $\tilde{\theta}^{(t)} = \theta^{(t-1)}$ which differ from $\theta^{(t)}$, the ones we apply them to. This is inherently due to the parallel

nature of our execution, and what we denote by "delayed update". Sec. 4.3 shows that this has drastic impacts on the convergence, despite being only delayed by one time step. We hypothesize that, although the delay is limited to $\tau = 1$ and the dependency on delay is known to be linear [67], the training dynamics differ significantly from those of the standard setting.

Weight Prediction (WP). Proposed by the work of [8] on mitigating pipeline delays, a simple estimation strategy is to reuse the most recently received gradients and apply a second optimizer step. Compared to DPU, this modifies the update rule for $\tilde{\theta}^{(t+1)}$, leading to:

$$g_i^{(t+1)} = \nabla F_i(\tilde{\theta}^{(t)}, \xi^{(t)})$$

$$\theta^{(t+1)} = \text{Opt} \left(\theta^{(t)}, \sum_{i=1}^N \frac{N_i}{\sum_i N_i} g_i^{(t)} \right), \quad \tilde{\theta}^{(t+1)} = \text{Opt} \left(\theta^{(t+1)}, \sum_{i=1}^N \frac{N_i}{\sum_i N_i} g_i^{(t)} \right). \quad (\text{WP})$$

While this enables overlap by decoupling communication and computation, there is no formal guarantee that it leads to favorable convergence. We empirically evaluate this method in Sec. 4.3, and observe that its training dynamics deviate from the DDP baseline—unlike ACCO.

3.2 ACCO: a structured approach to Communication-Computation overlap.

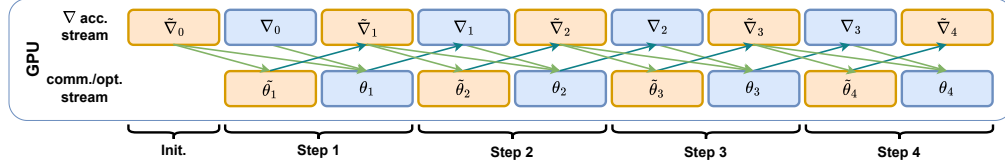


Figure 2: ACCO’s two-stage mechanism (1)-(2) to compensate the delayed updates via overlapping.

ACCO. ACCO splits the computation of the mini-batch gradients into two successive stages, where the first half of the mini-batch is used to estimate $\tilde{\theta}^{(t+1)}$ while $\theta^{(t+1)}$ is calculated using the entire mini-batch. This is further motivated by the fact that gradient accumulation can be used to reach the extremely large batch sizes required to train LLMs [84], and if gradients are computed *sequentially* on a worker, we can leverage this to produce our estimate. Thus, the two stages, as in Fig. 2, are

$$(1) \begin{cases} g_i^{(t)} = \nabla F_i(\theta^{(t)}, \xi^{(t)}), \\ \tilde{\theta}^{(t+1)} = \text{Opt} \left(\theta^{(t)}, \sum_{i=1}^N \frac{N_i}{\sum_j N_j} \tilde{g}_i^{(t)} \right), \end{cases} \quad (2) \begin{cases} \tilde{g}_i^{(t+1)} = \nabla F_i(\tilde{\theta}^{(t+1)}, \tilde{\xi}^{(t)}), \\ \theta^{(t+1)} = \text{Opt} \left(\theta^{(t)}, \sum_{i=1}^N \frac{N_i}{2 \sum_j N_j} (g_i^{(t)} + \tilde{g}_i^{(t)}) \right), \end{cases} \quad (\text{ACCO})$$

We next describe the different components, whose streams can be run in parallel:

- (1) The computation stream uses the second half of the mini-batch to compute the gradients $g_i^{(t)}$ with respect to parameters $\theta^{(t)}$ while the communication stream estimates what would be the next steps parameters $\tilde{\theta}^{(t+1)}$ using the estimated gradients $\tilde{g}_i^{(t)}$.
- (2) The computation stream uses the first half of the mini-batch to estimate what would be the gradients $\tilde{g}_i^{(t+1)}$ of the next parameters $\theta^{(t+1)}$ using estimated parameters $\tilde{\theta}^{(t+1)}$ while the communication stream computes $\theta^{(t+1)}$ using the full mini-batch. Note that it starts from the same version of the parameters $\theta^{(t)}$ as in step (1). The first half $\tilde{g}_i^{(t)}$ was estimated at step (2) of the *last round*, while (1) compute the second half $g_i^{(t)}$.

Theoretical analysis of ACCO. We now state our main results (SGD, for simplicity), with complete proofs provided in the appendix. The key idea underlying all proofs is that, for any minimizer θ^* of f and any $\eta > 0$, the following function serves as a Lyapunov function for our dynamics

$$V(\theta, \tilde{\theta}) \triangleq f(\theta) - f(\theta^*) + \eta L(f(\tilde{\theta}) - f(\theta^*)) + L\|\theta - \tilde{\theta}\|^2 \geq 0.$$

Proposition 3.1 (GD). Let $f : \mathbb{R}^d \rightarrow \mathbb{R}$ be L -smooth and $\theta^* \in \arg \min f$. For $\eta \leq \frac{1}{2L}$, define

$$\theta_{t+1} = \theta_t - \frac{\eta}{2} \left(\nabla f(\theta_t) + \nabla f(\tilde{\theta}_t) \right), \quad \tilde{\theta}_{t+1} = \theta_t - \eta \nabla f(\tilde{\theta}_t).$$

Then, for any $T \geq 1$, and initializations $\theta_0, \tilde{\theta}_0 \in \mathbb{R}^d$, we have

$$\frac{1}{T} \sum_{t=0}^{T-1} \left(\|\nabla f(\theta_t)\|^2 + \|\nabla f(\tilde{\theta}_t)\|^2 \right) \leq \frac{8}{\eta T} \left(f(\theta_0) + f(\tilde{\theta}_0) - 2f(\theta^*) + L\|\theta_0 - \tilde{\theta}_0\|^2 \right).$$

Proposition 3.2 (SGD). *Under the same assumption as above, suppose $\theta_0 = \tilde{\theta}_0$ and we perform:*

$$\theta_{t+1} = \theta_t - \frac{\eta}{2}(g_t + \tilde{g}_t), \quad \tilde{\theta}_{t+1} = \theta_t - \eta \tilde{g}_t,$$

where g_t and \tilde{g}_t are unbiased, conditionally independent estimators of $\nabla f(\theta_t)$ and $\nabla f(\tilde{\theta}_t)$, respectively, with bounded variance σ^2 . Then, for $\eta \leq \frac{1}{2L}$ and any $T \geq 1$,

$$\frac{1}{T} \sum_{t=0}^{T-1} \mathbb{E} \left[\|\nabla f(\theta_t)\|^2 + \|\nabla f(\tilde{\theta}_t)\|^2 \right] \leq \frac{16}{\eta T} (f(\theta_0) - f(\theta^*)) + 8\sigma^2 L\eta.$$

We note that these rates recover the standard convergence guarantees of GD and SGD, unlike those in [75]. Indeed, unlike DPU or WP, ACCO does not rely on an approximation, which leads to a cleaner analysis and faster convergence, as reflected in our proof strategy. One can interpret DPU (with SGD as the optimizer Opt) as a parallel version of Delayed-SGD (D-SGD) with a one-step delay. While this setup has been shown to preserve asymptotic convergence rates in convex settings—such as quadratics [3] and strongly or quasi-convex functions [68]—our experiments (Sec. 4.3) show that, in practice, this delay significantly degrades performance when training LLMs with AdamW. In contrast, ACCO completely avoids delayed gradients, eliminating the impact of staleness. We note that the batch size in ACCO corresponds to the number of samples processed between two successive updates of θ . Although it uses a pair of stochastic gradients, $\nabla F(\theta^{(t)}, \xi^{(t)})$ and $\nabla F(\tilde{\theta}^{(t)}, \tilde{\xi}^{(t)})$, both are computed synchronously with respect to $\theta^{(t)}$ (see Fig. 2). We confirm this advantage in Sec. 4, where ACCO yields training curves nearly indistinguishable from those of DDP (see Figs. 6, 5, 7).

4 Experiments

In this section, we present our experiments. Section 4.2 details the shared experimental setup. In Sec. 4.3, we demonstrate the shortcomings of DPU and WP—initially discussed in Sec. 3—which motivate the design of ACCO. This initial analysis focuses on small language models and datasets, using *TinyStories* [16] as a testbed. Sec. 4.4 shows that ACCO scales effectively by training a 125M-parameter GPT-Neo [6] on OpenWebText [21]. Sec. 4.5 pushes further with instruction tuning of a 2.7B GPT-Neo model, emphasizing communication bottlenecks and the benefits of ACCO. Finally, Sec. 4.6 compares ACCO and DDP on heterogeneous hardware, where ACCO lets faster GPUs accumulate updates while waiting—unlike DDP—resulting in faster gradient computation.

4.1 Empirical motivation for ACCO

We first illustrate that the time spent communicating gradients can quickly trump the one used for computing them when using standard AdamW DDP to train LLMs. For that, we measure the time necessary to perform a full backward pass on a Llama-2 model [71] with 7B parameters hosted on a single GPU, using a batch size maxing out its memory. We compare this to the time necessary to compute an All-Reduce on those gradients with NCCL, varying the number of distributed workers. We experiment

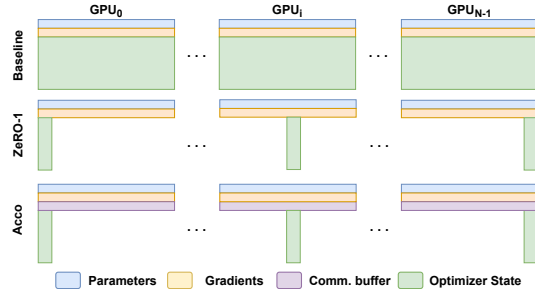


Figure 3: Memory requirements of ACCO vs DDP and ZeRO-1, see Tab.1 for quantitative details.

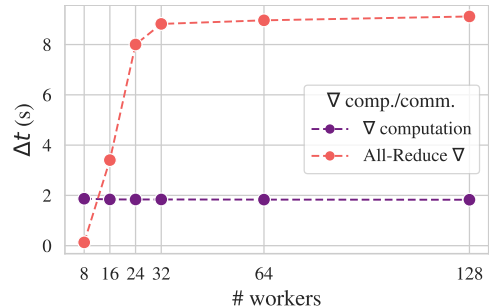


Figure 4: Time (per worker) spent computing and averaging gradients of a Llama-2 7B model for different numbers of GPUs.

on our local cluster of NVIDIA A100-80GB GPUs with 8 GPUs per node and an Omni-Path inter-connection network at 100 Gb/s for inter-node connections, intra-node connections being done with NVLink 300 GB/s. Each worker is hosted on a single GPU. Fig. 4 shows that the communication time outside of a GPU node in our cluster to average the gradients across workers can take more than $4\times$ the one spent on the whole forward and backward step. As DDP only partially hides communications during the backward [31], this means that our GPUs remain idle the majority of the time when we use more than 24 distributed workers, motivating the need for methods leveraging this time to compute.

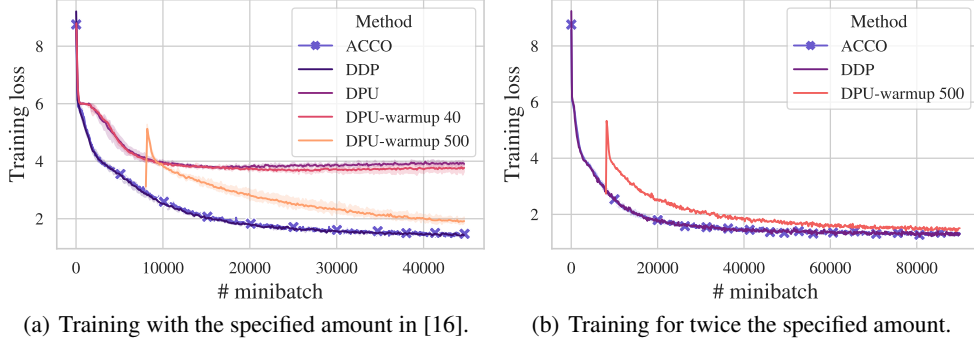


Figure 5: Impact of the delayed update and warmup steps.

4.2 Experimental setup

Our experiments are performed on the GPU cluster described in Sec. 4.1. A detailed pseudo-code for ACCO can be found in App. B.2. Our code is in PyTorch [52], and we verified that our implementation produces two different streams running in parallel for the computations and communications using NVIDIA’s Nsight System to profile it, shown in Fig. 13. We trained all our models with AdamW [36], using mixed precision: our model parameters, gradient accumulation and communication buffers are in `bf16` [24] while our sharded optimizer states are in single precision (see Fig. 3). As nowadays all distributed frameworks training LLMs at scale use a form of partitioning due to GPU memory constraints [58, 2], our main baseline is PyTorch’s DDP [31] with ZeRO-1 [55] to shard the optimizer’s state. As justified in Tab. 1, local optimization methods cannot be realistically considered for memory reasons. To compare in good faith DPU to ACCO in terms of wall-clock time, we also implemented our own version of DPU, as the implementation [61] solves a different problem than ours. The original ZeRO does not overlap computation and communication as it is designed to host the optimizer on the CPU, and is slower than ZeRO due to CPU and GPU memory transfers [60].

4.3 ACCO on TinyStories

We experiment with small language models on the TinyStories dataset [16], closely following their configuration and training hyperparameters. We use a 36M-parameter GPT-Neo-based [6] decoder-only transformer and train a BPE tokenizer on TinyStories to match their 10k vocabulary. All experiments are run with 8 workers on a single node.

Impact of delayed updates. First, we investigate the impact of using delayed updates, re-purposing DPU [60] as described in Sec. 3. We run three variants of this algorithm: (1) with no warmup, (2) with 40 warmup steps of non-delayed optimization step before switching to DPU (done in [60]), and (3) with 500 steps of warmup. We report in Fig. 5 our training losses on 8 distributed workers averaged over 3 runs. Using delayed updates greatly hurts convergence, especially when no or too few warmup steps are performed. Surprisingly, the number of warmup steps given in [60] does not work here, hinting that it is a sensitive hyper-parameter to tune for each use-case. If we train for twice as long as specified in [16], then the DPU training curve approaches the baseline one, without totally catching it.

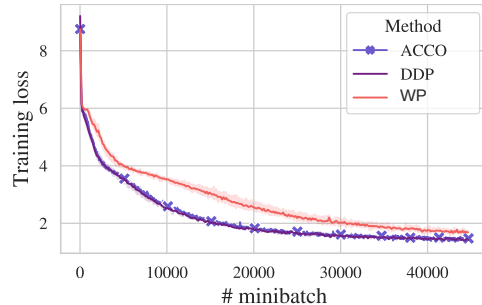
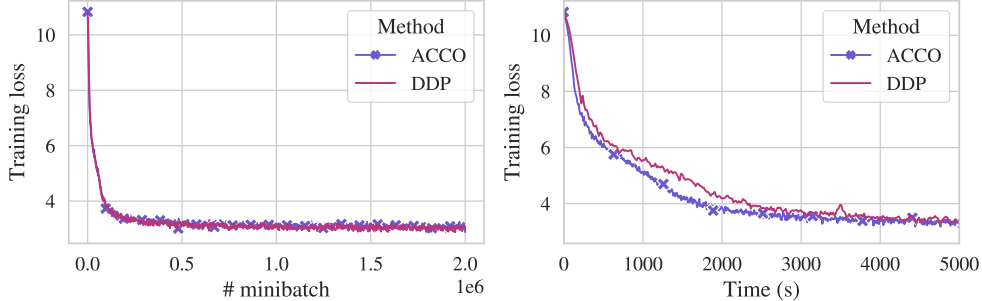


Figure 6: ACCO vs. WP on TinyStories

Contrary to this, the training curve of our algorithm ACCO perfectly matches DDP, as advocated by our theory.

Compensation via WP. To mitigate the detrimental impact of using delayed updates, we test a first approach to mitigate it: WP as described in Sec. 3. This method applies two consecutive optimizer steps, re-using twice the same mini-batch. The first step produces the usual updated parameters, while the second predicts the parameters of the next step so that gradients can be computed on this estimate rather than on a stale version of the model. In Fig. 6, we compare the training curves of this delay-compensation method to ours. We remark that, while ACCO perfectly matches the DDP baseline at all times, WP displays worse behavior, especially at the beginning of the training. Thus, we dismiss this method and keep ours for the remaining experiments.



(a) Evolution of the loss over the whole training. (b) Focus on the first part of the training w.r.t time.

Figure 7: Training curves for ACCO and DDP with 32 workers trained for 50B tokens.

4.4 Training GPT-Neo on OpenWebText

To assess how ACCO scales with larger models and more data, we pre-trained a model equivalent to GPT-2 [54] with both ACCO and DDP with a ZeRO optimizer. Specifically, we used the GPT-Neo architecture [6] with 125 million parameters and the OpenWebText dataset [21], which contains 40 GB of text. We used the GPT-Neo tokenizer, pre-trained on the Pile dataset [20]. The models were trained on sequences of 1024 tokens, with documents concatenated using end-of-sequence tokens. To assess the impact of using different hardware, the experiment was repeated on 2 different clusters. The first was conducted on 8 H100-PCIe 80GB on a single node. The second was on 32 A100-80G GPU distributed on 4 nodes. We maxed out the memory of our GPUs with a local mini-batch size of 24. To reach a sufficiently large overall batch size, we used 1 step of gradient accumulation for DDP, and none for ACCO as our method naturally accumulates over 1 step, resulting for the first and second experiments in respectively 400K and 1.5M tokens per effective batch for both ACCO and DDP. In Tab. 3, we report additional experimental details, and notice that training with ACCO allows for a 25% speedup on this pre-training task, which is additionally illustrated in Fig. 7. We also report that our implementation of ACCO adaptively scheduled 315 supplementary accumulation steps over the whole training to prevent GPUs from idling while waiting for communications. Further details and results for the H100 experiment can be found in App. A. Tab. 2 reports the perplexity of trained language models with both methods. We evaluate the perplexity of language models on LAMBADA [51] and a test split of OpenWebText, and report similar results for both methods.

Table 2: Perplexity of our trained LLMs

| Method | LAMBADA (ppl ↓) | OpenWebText (ppl ↓) |
|----------|-----------------|---------------------|
| ACCO 1x8 | 47.1 | 24.2 |
| DDP 1x8 | 47.5 | 24.3 |
| ACCO 4x8 | 45.5 | 22.5 |
| DDP 4x8 | 44.1 | 21.7 |

4.5 ACCO for instruction fine-tuning

In the former sections, we compared ACCO against DDP with ZeRO in the pre-training stage. To further validate our algorithm, we consider the GPT-Neo 2.7B model [6] pre-trained on the Pile dataset [20] and finetuned it on the Alpaca dataset [70] containing 52k pairs of instruction/answer. We fine-tuned the model using two configurations: 8 A100-80G on a single node, and 8 A100-80G distributed equally across 2 nodes. Samples are padded to match the longest sequence in the mini-

batch. We fixed the mini-batch size at 4, leading to a total batch size of 128 for all methods. For DDP and DPU, we used a gradient accumulation of 4, while for ACCO, a gradient accumulation of 2 to account for the ACCO accumulation described in Sec. 1. The learning rate was set to 2×10^{-5} , and with a warmup of 50 steps for DPU. In this setting, padding to the longest sequence in the mini-batch induces more variability in the number of tokens per mini-batch. This results in more variability in the computational load for each worker, leading to increased wait times for synchronization. We observe in Fig. 8 that ACCO achieves a low validation loss faster than DDP in both settings. Notably, the difference between ACCO DDP becomes more pronounced when workers are distributed across multiple nodes. Additionally, as shown in Tab. 3, larger models and optimizers result in longer communication times, further demonstrating the efficiency of ACCO in mitigating communication bottlenecks. This advantage translates to an 87% speedup for ACCO (see Tab. 3), highlighting the significant impact of communication bottlenecks on standard methods.

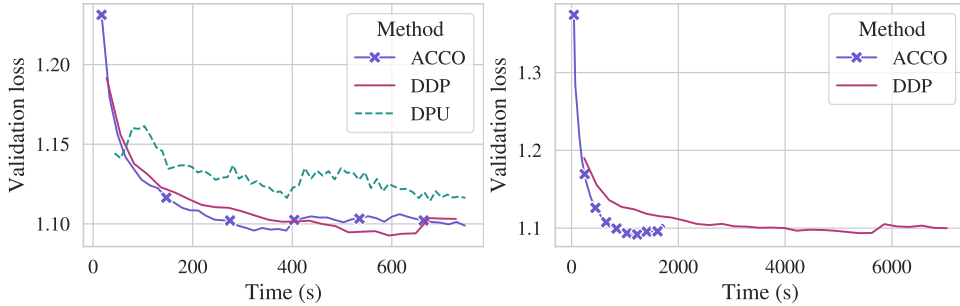


Figure 8: Validation curve with 8 workers on 1 node (left), and 4 workers/node on 2 nodes (right).

4.6 Experiment Using Heterogeneous Devices

To witness the impact of using heterogeneous devices, we run ACCO and compare it to DDP in a four workers setting, with one of the GPU four times slower than the other three. The training setting is the same as in Sec. 4.3. As we experiment on a A100 GPUs cluster, we simulate the heterogeneity of the hardware using the `time.sleep()` python command. First, we measure the time that a standard forward-backward step takes, and make one of the four GPUs idle for three times this amount after each forward-backward pass. In this context, DDP is only as fast as the slowest worker: 3 out of the 4 workers are idle 3/4 of the time. With ACCO, the other workers accumulate during the time they wait for the slow one to finish. Thus, ACCO allows to compute gradients for large batch sizes faster than standard baselines, resulting significantly smaller wall clock time, as shown in Fig. 9.

Table 3: Pre-training (PT) and finetuning (FT) time speedup with ACCO against DDP on various setups with GPT-Neo.

| Stage | Model | GPUs | #tokens | ZeRO-1 | ACCO |
|-------|-------|------|---------|--------|--------|
| PT | 125M | 1x8 | 6B | 4h41m | 4h25m |
| | | 4x8 | 50B | 14h41m | 10h55m |
| FT | 2.7B | 1x8 | 80M | 43min | 25min |
| | | 2x4 | 80M | 3h46m | 29min |

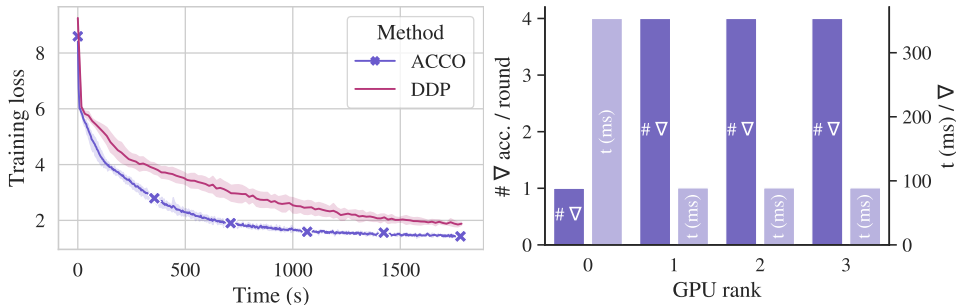


Figure 9: Training curves with 1 slow worker (4× slower).

Conclusion

ACCO is a novel algorithm that addresses both memory and communication bottlenecks in distributed LLM training, with provable guarantees which match standard SGD. By overlapping gradient computation and communication while partitioning optimizer states, ACCO reduces communication overhead in a memory-efficient way. A new two-stage compensation mechanism corrects for delayed updates, ensuring convergence comparable to standard optimizers—without requiring warmup. Empirical results show significant speedups across pre-training and fine-tuning tasks, particularly in multi-node and heterogeneous environments.

Acknowledgements

This work was supported by Project ANR-21-CE23-0030 ADONIS, EMERG-ADONIS from Alliance SU, PEPR IA (grant SHARP ANR-23-PEIA-0008), and the Sorbonne Center for Artificial Intelligence (SCAI) of Sorbonne University (IDEX SUPER 11-IDEX-0004). It was granted access to the AI resources of IDRIS under the allocation 2023-A0151014526 made by GENCI. EB acknowledges funding from FRQNT New Scholar and computational support from CFI.

References

- [1] Alekh Agarwal and John C Duchi. Distributed delayed stochastic optimization. In J. Shawe-Taylor, R. Zemel, P. Bartlett, F. Pereira, and K.Q. Weinberger, editors, *Advances in Neural Information Processing Systems*, volume 24. Curran Associates, Inc., 2011.
- [2] Alex Andonian, Quentin Anthony, Stella Biderman, Sid Black, Preetham Gali, Leo Gao, Eric Hallahan, Josh Levy-Kramer, Connor Leahy, Lucas Nestler, Kip Parker, Michael Pieler, Jason Phang, Shivanshu Purohit, Hailey Schoelkopf, Dashiell Stander, Tri Songz, Curt Tigges, Benjamin Thérien, Phil Wang, and Samuel Weinbach. GPT-NeoX: Large Scale Autoregressive Language Modeling in PyTorch, 9 2023.
- [3] Yossi Arjevani, Ohad Shamir, and Nathan Srebro. A tight convergence analysis for stochastic gradient descent with delayed updates. In Aryeh Kontorovich and Gergely Neu, editors, *Proceedings of the 31st International Conference on Algorithmic Learning Theory*, volume 117 of *Proceedings of Machine Learning Research*, pages 111–132. PMLR, 08 Feb–11 Feb 2020.
- [4] By Mahmoud Assran, Arda Aytikin, Hamid Reza Feyzmahdavian, Mikael Johansson, and Michael G. Rabbat. Advances in asynchronous parallel and distributed optimization. *Proceedings of the IEEE*, 108(11):2013–2031, 2020.
- [5] Mahmoud Assran, Nicolas Loizou, Nicolas Ballas, and Mike Rabbat. Stochastic gradient push for distributed deep learning. In Kamalika Chaudhuri and Ruslan Salakhutdinov, editors, *Proceedings of the 36th International Conference on Machine Learning*, volume 97 of *Proceedings of Machine Learning Research*, pages 344–353. PMLR, 09–15 Jun 2019.
- [6] Sid Black, Gao Leo, Phil Wang, Connor Leahy, and Stella Biderman. GPT-Neo: Large Scale Autoregressive Language Modeling with Mesh-Tensorflow, March 2021.
- [7] Zachary Charles, Gabriel Teston, Lucio Dery, Keith Rush, Nova Fallen, Zachary Garrett, Arthur Szlam, and Arthur Douillard. Communication-efficient language model training scales reliably and robustly: Scaling laws for diloco. *arXiv preprint arXiv:2503.09799*, 2025.
- [8] Chi-Chung Chen, Chia-Lin Yang, and Hsiang-Yun Cheng. Efficient and robust parallel dnn training through model parallelism on multi-gpu platform, 2019.
- [9] Tianqi Chen, Bing Xu, Chiyuan Zhang, and Carlos Guestrin. Training deep nets with sublinear memory cost, 2016.
- [10] Xiangyi Chen, Xiaoyun Li, and P. Li. Toward communication efficient adaptive gradient method. *Proceedings of the 2020 ACM-IMS on Foundations of Data Science Conference*, 2020.
- [11] Yangrui Chen, Cong Xie, Meng Ma, Juncheng Gu, Yanghua Peng, Haibin Lin, Chuan Wu, and Yibo Zhu. Sapipe: Staleness-aware pipeline for data parallel dnn training. *Advances in Neural Information Processing Systems*, 35:17981–17993, 2022.

- [12] Jeffrey Dean, Greg Corrado, Rajat Monga, Kai Chen, Matthieu Devin, Mark Mao, Marc' aurelio Ranzato, Andrew Senior, Paul Tucker, Ke Yang, Quoc Le, and Andrew Ng. Large scale distributed deep networks. In F. Pereira, C.J. Burges, L. Bottou, and K.Q. Weinberger, editors, *Advances in Neural Information Processing Systems*, volume 25. Curran Associates, Inc., 2012.
- [13] Michael Diskin, Alexey Bukhtiyarov, Max Ryabinin, Lucile Saulnier, Quentin Lhoest, Anton Sinitsin, Dmitry Popov, Dmitry Pyrkun, Maxim Kashirin, Alexander Borzunov, Albert Villanova del Moral, Denis Mazur, Ilia Kobelev, Yacine Jernite, Thomas Wolf, and Gennady Pekhimenko. Distributed deep learning in open collaborations. In A. Beygelzimer, Y. Dauphin, P. Liang, and J. Wortman Vaughan, editors, *Advances in Neural Information Processing Systems*, 2021.
- [14] Arthur Douillard, Qixuan Feng, Andrei A Rusu, Rachita Chhaparia, Yani Donchev, Adhiguna Kuncoro, Marc'Aurelio Ranzato, Arthur Szlam, and Jiajun Shen. Diloco: Distributed low-communication training of language models. *arXiv preprint arXiv:2311.08105*, 2023.
- [15] Sanghamitra Dutta, Jianyu Wang, and Gauri Joshi. Slow and stale gradients can win the race. *IEEE Journal on Selected Areas in Information Theory*, 2(3):1012–1024, 2021.
- [16] Ronen Eldan and Yuanzhi Li. Tinstories: How small can language models be and still speak coherent english?, 2023.
- [17] Mathieu Even, Raphaël Berthier, Francis Bach, Nicolas Flammarion, Hadrien Hendrikx, Pierre Gaillard, Laurent Massoulié, and Adrien Taylor. A continuized view on nesterov acceleration for stochastic gradient descent and randomized gossip. In A. Beygelzimer, Y. Dauphin, P. Liang, and J. Wortman Vaughan, editors, *Advances in Neural Information Processing Systems*, 2021.
- [18] Shiqing Fan, Yi Rong, Chen Meng, Zongyan Cao, Siyu Wang, Zhen Zheng, Chuan Wu, Guoping Long, Jun Yang, Lixue Xia, et al. Dapple: A pipelined data parallel approach for training large models. In *Proceedings of the 26th ACM SIGPLAN Symposium on Principles and Practice of Parallel Programming*, pages 431–445, 2021.
- [19] Hamid Reza Feyzmahdavian and Mikael Johansson. Asynchronous iterations in optimization: New sequence results and sharper algorithmic guarantees. *Journal of Machine Learning Research*, 24(158):1–75, 2023.
- [20] Leo Gao, Stella Biderman, Sid Black, Laurence Golding, Travis Hoppe, Charles Foster, Jason Phang, Horace He, Anish Thite, Noa Nabeshima, et al. The pile: An 800gb dataset of diverse text for language modeling. *arXiv preprint arXiv:2101.00027*, 2020.
- [21] Aaron Gokaslan, Vanya Cohen, Ellie Pavlick, and Stefanie Tellex. Openwebtext corpus. <http://Skyllion007.github.io/OpenWebTextCorpus>, 2019.
- [22] Yanping Huang, Youlong Cheng, Ankur Bapna, Orhan Firat, Dehao Chen, Mia Chen, HyoukJoong Lee, Jiquan Ngiam, Quoc V Le, Yonghui Wu, et al. Gpipe: Efficient training of giant neural networks using pipeline parallelism. *Advances in neural information processing systems*, 32, 2019.
- [23] Jörn-Henrik Jacobsen, Arnold W.M. Smeulders, and Edouard Oyallon. i-revnet: Deep invertible networks. In *International Conference on Learning Representations*, 2018.
- [24] Dhiraj Kalamkar, Dheevatsa Mudigere, Naveen Mellempudi, Dipankar Das, Kunal Banerjee, Sasikanth Avancha, Dharma Teja Vooturi, Nataraj Jammalamadaka, Jianyu Huang, Hector Yuen, Jiyan Yang, Jongsoo Park, Alexander Heinecke, Evangelos Georganas, Sudarshan Srinivasan, Abhisek Kundu, Misha Smelyanskiy, Bharat Kaul, and Pradeep Dubey. A study of bfloat16 for deep learning training, 2019.
- [25] Sai Praneeth Karimireddy, Martin Jaggi, Satyen Kale, Mehryar Mohri, Sashank J. Reddi, Sebastian U. Stich, and Ananda Theertha Suresh. Mime: Mimicking centralized stochastic algorithms in federated learning. *ArXiv*, abs/2008.03606, 2020.
- [26] Chiheon Kim, Heungsub Lee, Myungryong Jeong, Woonhyuk Baek, Boogyeon Yoon, Ildoo Kim, Sungbin Lim, and Sungwoong Kim. torchgpipe: On-the-fly pipeline parallelism for training giant models, 2020.
- [27] Diederik Kingma and Jimmy Ba. Adam: A method for stochastic optimization. In *International Conference on Learning Representations (ICLR)*, San Diego, CA, USA, 2015.
- [28] Anastasia Koloskova, Sebastian U. Stich, and Martin Jaggi. Sharper convergence guarantees for asynchronous sgd for distributed and federated learning. In *Proceedings of the 36th International*

Conference on Neural Information Processing Systems, NIPS '22, Red Hook, NY, USA, 2024. Curran Associates Inc.

- [29] Jakub Konečný, H. B. McMahan, Daniel Ramage, and Peter Richtárik. Federated optimization: Distributed machine learning for on-device intelligence. *ArXiv*, abs/1610.02527, 2016.
- [30] Atli Kosson, Vitaliy Chiley, Abhinav Venigalla, Joel Hestness, and Urs Köster. Pipelined backpropagation at scale: Training large models without batches, 2021.
- [31] Shen Li, Yanli Zhao, Rohan Varma, Omkar Salpekar, Pieter Noordhuis, Teng Li, Adam Paszke, Jeff Smith, Brian Vaughan, Pritam Damania, and Soumith Chintala. Pytorch distributed: experiences on accelerating data parallel training. *Proc. VLDB Endow.*, 13(12):3005–3018, aug 2020.
- [32] Tian Li, Anit Kumar Sahu, Manzil Zaheer, Maziar Sanjabi, Ameet Talwalkar, and Virginia Smith. Federated optimization for heterogeneous networks. In *ICML Workshop on Adaptive & Multitask Learning: Algorithms & Systems*, 2019.
- [33] Youjie Li, Mingchao Yu, Songze Li, Salman Avestimehr, Nam Sung Kim, and Alexander Schwing. Pipe-sgd: A decentralized pipelined sgd framework for distributed deep net training. *Advances in Neural Information Processing Systems*, 31, 2018.
- [34] Tao Lin, Sebastian U. Stich, Kumar Kshitij Patel, and Martin Jaggi. Don’t use large mini-batches, use local sgd. In *International Conference on Learning Representations*, 2020.
- [35] Yuliang Liu, Shenggui Li, Jiarui Fang, Yanjun Shao, Boyuan Yao, and Yang You. Colossal-auto: Unified automation of parallelization and activation checkpoint for large-scale models, 2023.
- [36] Ilya Loshchilov and Frank Hutter. Decoupled weight decay regularization. In *International Conference on Learning Representations*, 2019.
- [37] Karttikeya Mangalam, Haoqi Fan, Yanghao Li, Chao-Yuan Wu, Bo Xiong, Christoph Feichtenhofer, and Jitendra Malik. Reversible vision transformers. In *Proceedings of the IEEE/CVF Conference on Computer Vision and Pattern Recognition*, pages 10830–10840, 2022.
- [38] Artavazd Maranjyan, Mher Safaryan, and Peter Richtárik. Gradskip: Communication-accelerated local gradient methods with better computational complexity, 2022.
- [39] Ryan McDonald, Keith Hall, and Gideon Mann. Distributed training strategies for the structured perceptron. In *Human Language Technologies: The 2010 Annual Conference of the North American Chapter of the Association for Computational Linguistics*, HLT '10, page 456–464, USA, 2010. Association for Computational Linguistics.
- [40] Brendan McMahan, Eider Moore, Daniel Ramage, Seth Hampson, and Blaise Agüera y Arcas. Communication-Efficient Learning of Deep Networks from Decentralized Data. In Aarti Singh and Jerry Zhu, editors, *Proceedings of the 20th International Conference on Artificial Intelligence and Statistics*, volume 54 of *Proceedings of Machine Learning Research*, pages 1273–1282. PMLR, 20–22 Apr 2017.
- [41] Konstantin Mishchenko, Francis Bach, Mathieu Even, and Blake Woodworth. Asynchronous SGD beats minibatch SGD under arbitrary delays. In Alice H. Oh, Alekh Agarwal, Danielle Belgrave, and Kyunghyun Cho, editors, *Advances in Neural Information Processing Systems*, 2022.
- [42] Konstantin Mishchenko, Grigory Malinovsky, Sebastian Stich, and Peter Richtárik. Proxskip: Yes! local gradient steps provably lead to communication acceleration! finally! *arXiv preprint arXiv:2202.09357*, 2022.
- [43] Ioannis Mitliagkas, Ce Zhang, Stefan Hadjis, and Christopher Ré. Asynchrony begets momentum, with an application to deep learning. In *2016 54th Annual Allerton Conference on Communication, Control, and Computing (Allerton)*, page 997–1004. IEEE Press, 2016.
- [44] Adel Nabli, Eugene Belilovsky, and Edouard Oyallon. $\mathcal{A}^2\text{CiD}^2$: Accelerating asynchronous communication in decentralized deep learning. In *Thirty-seventh Conference on Neural Information Processing Systems*, 2023.
- [45] Adel Nabli and Edouard Oyallon. DADAO: Decoupled accelerated decentralized asynchronous optimization. In Andreas Krause, Emma Brunskill, Kyunghyun Cho, Barbara Engelhardt, Sivan Sabato, and Jonathan Scarlett, editors, *Proceedings of the 40th International Conference on Machine Learning*, volume 202 of *Proceedings of Machine Learning Research*, pages 25604–25626. PMLR, 23–29 Jul 2023.

- [46] Giorgi Nadiradze, Ilia Markov, Bapi Chatterjee, Vyacheslav Kungurtsev, and Dan Alistarh. Elastic consistency: A practical consistency model for distributed stochastic gradient descent. 2021.
- [47] Deepak Narayanan, Aaron Harlap, Amar Phanishayee, Vivek Seshadri, Nikhil R Devanur, Gregory R Ganger, Phillip B Gibbons, and Matei Zaharia. Pipedream: Generalized pipeline parallelism for dnn training. In *Proceedings of the 27th ACM Symposium on Operating Systems Principles*, pages 1–15, 2019.
- [48] Deepak Narayanan, Amar Phanishayee, Kaiyu Shi, Xie Chen, and Matei Zaharia. Memory-efficient pipeline-parallel dnn training. In *International Conference on Machine Learning*, pages 7937–7947. PMLR, 2021.
- [49] John Nguyen, Kshitiz Malik, Hongyuan Zhan, Ashkan Yousefpour, Mike Rabbat, Mani Malek, and Dzmitry Huba. Federated learning with buffered asynchronous aggregation. In Gustavo Camps-Valls, Francisco J. R. Ruiz, and Isabel Valera, editors, *Proceedings of The 25th International Conference on Artificial Intelligence and Statistics*, volume 151 of *Proceedings of Machine Learning Research*, pages 3581–3607. PMLR, 28–30 Mar 2022.
- [50] Jose Javier Gonzalez Ortiz, Jonathan Frankle, Mike Rabbat, Ari Morcos, and Nicolas Ballas. Trade-offs of local sgd at scale: An empirical study. In *NeurIPS 2020 OptML Workshop*, 2021.
- [51] Denis Paperno, Germán Kruszewski, Angeliki Lazaridou, Ngoc Quan Pham, Raffaella Bernardi, Sandro Pezzelle, Marco Baroni, Gemma Boleda, and Raquel Fernandez. The LAMBADA dataset: Word prediction requiring a broad discourse context. In *Proceedings of the 54th Annual Meeting of the Association for Computational Linguistics (Volume 1: Long Papers)*, pages 1525–1534, Berlin, Germany, August 2016. Association for Computational Linguistics.
- [52] Adam Paszke, Sam Gross, Francisco Massa, Adam Lerer, James Bradbury, Gregory Chanan, Trevor Killeen, Zeming Lin, Natalia Gimelshein, Luca Antiga, Alban Desmaison, Andreas Köpf, Edward Yang, Zach DeVito, Martin Raison, Alykhan Tejani, Sasank Chilamkurthy, Benoit Steiner, Lu Fang, Junjie Bai, and Soumith Chintala. Pytorch: an imperative style, high-performance deep learning library. In *Proceedings of the 33rd International Conference on Neural Information Processing Systems*, Red Hook, NY, USA, 2019. Curran Associates Inc.
- [53] Suchita Pati, Shaizeen Aga, Mahzabeen Islam, Nuwan Jayasena, and Matthew D. Sinclair. Computation vs. communication scaling for future transformers on future hardware, 2023.
- [54] Alec Radford, Jeff Wu, Rewon Child, David Luan, Dario Amodei, and Ilya Sutskever. Language models are unsupervised multitask learners. 2019.
- [55] Samyam Rajbhandari, Jeff Rasley, Olatunji Ruwase, and Yuxiong He. Zero: memory optimizations toward training trillion parameter models. In *Proceedings of the International Conference for High Performance Computing, Networking, Storage and Analysis, SC '20*. IEEE Press, 2020.
- [56] Samyam Rajbhandari, Jeff Rasley, Olatunji Ruwase, and Yuxiong He. Zero: Memory optimizations toward training trillion parameter models, 2020.
- [57] Samyam Rajbhandari, Olatunji Ruwase, Jeff Rasley, Shaden Smith, and Yuxiong He. Zero-infinity: Breaking the gpu memory wall for extreme scale deep learning, 2021.
- [58] Jeff Rasley, Samyam Rajbhandari, Olatunji Ruwase, and Yuxiong He. Deepspeed: System optimizations enable training deep learning models with over 100 billion parameters. In *Proceedings of the 26th ACM SIGKDD International Conference on Knowledge Discovery & Data Mining, KDD '20*, page 3505–3506, New York, NY, USA, 2020. Association for Computing Machinery.
- [59] Sashank J. Reddi, Zachary Charles, Manzil Zaheer, Zachary Garrett, Keith Rush, Jakub Konečný, Sanjiv Kumar, and Hugh Brendan McMahan. Adaptive federated optimization. In *International Conference on Learning Representations*, 2021.
- [60] Jie Ren, Samyam Rajbhandari, Reza Yazdani Aminabadi, Olatunji Ruwase, Shuangyan Yang, Minjia Zhang, Dong Li, and Yuxiong He. Zero-offload: Democratizing billion-scale model training, 2021.
- [61] Jie Ren, Samyam Rajbhandari, Reza Yazdani Aminabadi, Olatunji Ruwase, Shuangyan Yang, Minjia Zhang, Dong Li, and Yuxiong He. <https://github.com/microsoft/deepspeed/discussions/2461>, 2022.

- [62] Stephane Rivaud, Louis Fournier, Thomas Pumis, Eugene Belilovsky, Michael Eickenberg, and Edouard Oyallon. PETRA: Parallel end-to-end training with reversible architectures. In *The Thirteenth International Conference on Learning Representations*, 2025.
- [63] Shuheng Shen, Linli Xu, Jingchang Liu, Xianfeng Liang, and Yifei Cheng. Faster distributed deep net training: computation and communication decoupled stochastic gradient descent. In *Proceedings of the 28th International Joint Conference on Artificial Intelligence*, page 4582–4589. AAAI Press, 2019.
- [64] Mohammad Shoeybi, Mostofa Patwary, Raul Puri, Patrick LeGresley, Jared Casper, and Bryan Catanzaro. Megatron-lm: Training multi-billion parameter language models using model parallelism. *arXiv preprint arXiv:1909.08053*, 2019.
- [65] Shaden Smith, Mostofa Patwary, Brandon Norick, Patrick LeGresley, Samyam Rajbhandari, Jared Casper, Zhun Liu, Shrimai Prabhumoye, George Zerveas, Vijay Korthikanti, et al. Using deepspeed and megatron to train megatron-turing nlq 530b, a large-scale generative language model. *arXiv preprint arXiv:2201.11990*, 2022.
- [66] Sebastian U. Stich. Local SGD converges fast and communicates little. In *International Conference on Learning Representations*, 2019.
- [67] Sebastian U. Stich and Sai Praneeth Karimireddy. The error-feedback framework: better rates for sgd with delayed gradients and compressed updates. *Journal of Machine Learning Research*, 21(1), jan 2020.
- [68] Sebastian U. Stich and Sai Praneeth Karimireddy. The error-feedback framework: better rates for sgd with delayed gradients and compressed updates. *J. Mach. Learn. Res.*, 21(1), January 2020.
- [69] Weigao Sun, Zhen Qin, Weixuan Sun, Shidi Li, Dong Li, Xuyang Shen, Yu Qiao, and Yiran Zhong. CO2: Efficient distributed training with full communication-computation overlap. In *The Twelfth International Conference on Learning Representations*, 2024.
- [70] Rohan Taori, Ishaan Gulrajani, Tianyi Zhang, Yann Dubois, Xuechen Li, Carlos Guestrin, Percy Liang, and Tatsunori B. Hashimoto. Stanford alpaca: An instruction-following llama model. https://github.com/tatsu-lab/stanford_alpaca, 2023.
- [71] Hugo Touvron, Louis Martin, Kevin Stone, Peter Albert, Amjad Almahairi, Yasmine Babaei, Nikolay Bashlykov, Soumya Batra, Prajjwal Bhargava, Shruti Bhosale, Dan Bikel, Lukas Blecher, Cristian Canton Ferrer, Moya Chen, Guillem Cucurull, David Esiobu, Jude Fernandes, Jeremy Fu, Wenyin Fu, Brian Fuller, Cynthia Gao, Vedanuj Goswami, Naman Goyal, Anthony Hartshorn, Saghar Hosseini, Rui Hou, Hakan Inan, Marcin Kardas, Viktor Kerkez, Madian Khabsa, Isabel Kloumann, Artem Korenev, Punit Singh Koura, Marie-Anne Lachaux, Thibaut Lavril, Jenya Lee, Diana Liskovich, Yinghai Lu, Yuning Mao, Xavier Martinet, Todor Mihaylov, Pushkar Mishra, Igor Molybog, Yixin Nie, Andrew Poulton, Jeremy Reizenstein, Rashi Rungta, Kalyan Saladi, Alan Schelten, Ruan Silva, Eric Michael Smith, Ranjan Subramanian, Xiaoqing Ellen Tan, Binh Tang, Ross Taylor, Adina Williams, Jian Xiang Kuan, Puxin Xu, Zheng Yan, Iliyan Zarov, Yuchen Zhang, Angela Fan, Melanie Kambadur, Sharan Narang, Aurelien Rodriguez, Robert Stojnic, Sergey Edunov, and Thomas Scialom. Llama 2: Open foundation and fine-tuned chat models, 2023.
- [72] Ashish Vaswani, Noam Shazeer, Niki Parmar, Jakob Uszkoreit, Llion Jones, Aidan N Gomez, Łukasz Kaiser, and Illia Polosukhin. Attention is all you need. In I. Guyon, U. Von Luxburg, S. Bengio, H. Wallach, R. Fergus, S. Vishwanathan, and R. Garnett, editors, *Advances in Neural Information Processing Systems*, volume 30. Curran Associates, Inc., 2017.
- [73] Guanhua Wang, Heyang Qin, Sam Ade Jacobs, Connor Holmes, Samyam Rajbhandari, Olatunji Ruwase, Feng Yan, Lei Yang, and Yuxiong He. Zero++: Extremely efficient collective communication for giant model training, 2023.
- [74] Jianyu Wang, Hao Liang, and Gauri Joshi. Overlap local-sgd: An algorithmic approach to hide communication delays in distributed sgd. In *ICASSP 2020 - 2020 IEEE International Conference on Acoustics, Speech and Signal Processing (ICASSP)*. IEEE, May 2020.
- [75] Jianyu Wang, Vinayak Tania, Nicolas Ballas, and Michael Rabbat. Slowmo: Improving communication-efficient distributed sgd with slow momentum. In *International Conference on Learning Representations*, 2020.

- [76] Blake Woodworth, Kumar Kshitij Patel, Sebastian Stich, Zhen Dai, Brian Bullins, Brendan McMahan, Ohad Shamir, and Nathan Srebro. Is local SGD better than minibatch SGD? In Hal Daumé III and Aarti Singh, editors, *Proceedings of the 37th International Conference on Machine Learning*, volume 119 of *Proceedings of Machine Learning Research*, pages 10334–10343. PMLR, 13–18 Jul 2020.
- [77] Xuyang Wu, Sindri Magnusson, Hamid Reza Feyzmahdavian, and Mikael Johansson. Delay-adaptive step-sizes for asynchronous learning. In Kamalika Chaudhuri, Stefanie Jegelka, Le Song, Csaba Szepesvari, Gang Niu, and Sivan Sabato, editors, *Proceedings of the 39th International Conference on Machine Learning*, volume 162 of *Proceedings of Machine Learning Research*, pages 24093–24113. PMLR, 17–23 Jul 2022.
- [78] Cong Xie, Sanmi Koyejo, and Indranil Gupta. Asynchronous federated optimization. In *NeurIPS 2020 OptML Workshop*, 2020.
- [79] Bowen Yang, Jian Zhang, Jonathan Li, Christopher Re, Christopher Aberger, and Christopher De Sa. Pipemare: Asynchronous pipeline parallel dnn training. In A. Smola, A. Dimakis, and I. Stoica, editors, *Proceedings of Machine Learning and Systems*, volume 3, pages 269–296, 2021.
- [80] Bowen Yang, Jian Zhang, Jonathan Li, Christopher Ré, Christopher R. Aberger, and Christopher De Sa. Pipemare: Asynchronous pipeline parallel dnn training, 2020.
- [81] Jian Zhang and Ioannis Mitliagkas. Yellowfin and the art of momentum tuning. In A. Talwalkar, V. Smith, and M. Zaharia, editors, *Proceedings of Machine Learning and Systems*, volume 1, pages 289–308, 2019.
- [82] Sixin Zhang, Anna Choromanska, and Yann LeCun. Deep learning with elastic averaging sgd. In *Proceedings of the 28th International Conference on Neural Information Processing Systems - Volume 1*, NIPS’15, page 685–693, Cambridge, MA, USA, 2015. MIT Press.
- [83] Zhen Zhang, Shuai Zheng, Yida Wang, Justin Chiu, George Karypis, Trishul Chilimbi, Mu Li, and Xin Jin. Mics: Near-linear scaling for training gigantic model on public cloud, 2022.
- [84] Wayne Xin Zhao, Kun Zhou, Junyi Li, Tianyi Tang, Xiaolei Wang, Yupeng Hou, Yingqian Min, Beichen Zhang, Junjie Zhang, Zican Dong, Yifan Du, Chen Yang, Yushuo Chen, Zhipeng Chen, Jinhao Jiang, Ruiyang Ren, Yifan Li, Xinyu Tang, Zikang Liu, Peiyu Liu, Jian-Yun Nie, and Ji-Rong Wen. A survey of large language models, 2023.
- [85] Yanli Zhao, Andrew Gu, Rohan Varma, Liang Luo, Chien-Chin Huang, Min Xu, Less Wright, Hamid Shojanazeri, Myle Ott, Sam Shleifer, Alban Desmaison, Can Balioglu, Pritam Damania, Bernard Nguyen, Geeta Chauhan, Yuchen Hao, Ajit Mathews, and Shen Li. Pytorch fsdp: Experiences on scaling fully sharded data parallel, 2023.
- [86] Shuxin Zheng, Qi Meng, Taifeng Wang, Wei Chen, Nenghai Yu, Zhi-Ming Ma, and Tie-Yan Liu. Asynchronous stochastic gradient descent with delay compensation. In *Proceedings of the 34th International Conference on Machine Learning - Volume 70*, ICML’17, page 4120–4129. JMLR.org, 2017.
- [87] Fan Zhou and Guojing Cong. On the convergence properties of a k-step averaging stochastic gradient descent algorithm for nonconvex optimization. In *Proceedings of the Twenty-Seventh International Joint Conference on Artificial Intelligence, IJCAI-18*, pages 3219–3227. International Joint Conferences on Artificial Intelligence Organization, 7 2018.
- [88] Huiping Zhuang, Zhiping Lin, and Kar-Ann Toh. Accumulated decoupled learning: Mitigating gradient staleness in inter-layer model parallelization. *arXiv preprint arXiv:2012.03747*, 2020.
- [89] Huiping Zhuang, Yi Wang, Qinglai Liu, and Zhiping Lin. Fully decoupled neural network learning using delayed gradients. *IEEE transactions on neural networks and learning systems*, 33(10):6013–6020, 2021.
- [90] Martin Zinkevich, Markus Weimer, Lihong Li, and Alex Smola. Parallelized stochastic gradient descent. In J. Lafferty, C. Williams, J. Shawe-Taylor, R. Zemel, and A. Culotta, editors, *Advances in Neural Information Processing Systems*, volume 23. Curran Associates, Inc., 2010.

NeurIPS Paper Checklist

1. Claims

Question: Do the main claims made in the abstract and introduction accurately reflect the paper’s contributions and scope?

Answer: [\[Yes\]](#)

Justification: The introduction and abstract clearly state the goals and contributions of ACCO, which are substantiated through both theoretical analysis (Section 3) and experiments (Sections 4.3–4.6).

Guidelines:

- The answer NA means that the abstract and introduction do not include the claims made in the paper.
- The abstract and/or introduction should clearly state the claims made, including the contributions made in the paper and important assumptions and limitations. A No or NA answer to this question will not be perceived well by the reviewers.
- The claims made should match theoretical and experimental results, and reflect how much the results can be expected to generalize to other settings.
- It is fine to include aspirational goals as motivation as long as it is clear that these goals are not attained by the paper.

2. Limitations

Question: Does the paper discuss the limitations of the work performed by the authors?

Answer: [\[Yes\]](#)

Justification: For instance, Table 1 discusses the tradeoffs of each method.

Guidelines:

- The answer NA means that the paper has no limitation while the answer No means that the paper has limitations, but those are not discussed in the paper.
- The authors are encouraged to create a separate “Limitations” section in their paper.
- The paper should point out any strong assumptions and how robust the results are to violations of these assumptions (e.g., independence assumptions, noiseless settings, model well-specification, asymptotic approximations only holding locally). The authors should reflect on how these assumptions might be violated in practice and what the implications would be.
- The authors should reflect on the scope of the claims made, e.g., if the approach was only tested on a few datasets or with a few runs. In general, empirical results often depend on implicit assumptions, which should be articulated.
- The authors should reflect on the factors that influence the performance of the approach.
- The authors should discuss the computational efficiency of the proposed algorithms and how they scale with dataset size.
- If applicable, the authors should discuss possible limitations of their approach to address problems of privacy and fairness.

3. Theory assumptions and proofs

Question: For each theoretical result, does the paper provide the full set of assumptions and a complete (and correct) proof?

Answer: [\[Yes\]](#)

Justification: Section 3 provides the assumptions and sketches of the proofs; full convergence analysis and Lyapunov function details are referenced and further elaborated in the appendix.

Guidelines:

- The answer NA means that the paper does not include theoretical results.
- All the theorems, formulas, and proofs in the paper should be numbered and cross-referenced.
- All assumptions should be clearly stated or referenced in the statement of any theorems.

- Proofs can appear in the main paper or the supplemental material; if in supplemental material, include a short proof sketch in the main text.
- Theorems and Lemmas relied upon should be properly referenced.

4. Experimental result reproducibility

Question: Does the paper fully disclose all the information needed to reproduce the main experimental results of the paper (regardless of whether the code and data are provided or not)?

Answer: [Yes]

Justification: Section 4.2 describes the full environment and configurations, including model architecture, hardware specs, optimizer, precision formats, and batch sizes. Details are further supported by Appendix sections and figures.

Guidelines:

- The answer NA means that the paper does not include experiments.
- If the contribution is a dataset and/or model, the authors should describe the steps taken to make results reproducible or verifiable.
- Depending on the contribution, reproducibility may require full architecture details, commands, or hosted access; see NeurIPS policy for options.

5. Open access to data and code

Question: Does the paper provide open access to the data and code, with sufficient instructions to faithfully reproduce the main experimental results, as described in supplemental material?

Answer: [Yes]

Justification: The paper states that the code will be released in a public open-source repository at publication time (end of Introduction). All datasets used are publicly available.

Guidelines:

- See NeurIPS code/data submission guidelines (<https://nips.cc/public/guides/CodeSubmissionPolicy>).
- Include exact commands and environment when feasible; anonymize at submission time if applicable.

6. Experimental setting/details

Question: Does the paper specify all the training and test details (e.g., data splits, hyperparameters, how they were chosen, type of optimizer, etc.) necessary to understand the results?

Answer: [Yes]

Justification: Sections 4.2, 4.3, 4.4, and 4.5 specify training configurations, datasets, optimizer, batch sizes, accumulation strategies, and evaluation metrics.

Guidelines:

- Core details should appear in the paper; full details can be in code, appendix, or supplemental material.

7. Experiment statistical significance

Question: Does the paper report error bars suitably and correctly defined or other appropriate information about the statistical significance of the experiments?

Answer: [Yes]

Justification: For TinyStories experiments, results are averaged over 3 runs (see Section 4.3); trends are visualized. For large-scale runs, we show consistent convergence behavior.

Guidelines:

- Clearly state what variability factors error bars capture and how they are computed.
- Clarify whether bars are standard deviation or standard error; use asymmetric bars when appropriate.

8. Experiments compute resources

Question: For each experiment, does the paper provide sufficient information on the computer resources (type of compute workers, memory, time of execution) needed to reproduce the experiments?

Answer: [Yes]

Justification: Section 4.2 specifies compute resources including GPU model, memory, interconnect bandwidths, and training durations (see also Table 3).

Guidelines:

- Indicate worker type (CPU/GPU), cluster/cloud details, memory/storage.
- Provide per-run and total compute estimates when feasible.

9. Code of ethics

Question: Does the research conducted in the paper conform, in every respect, with the NeurIPS Code of Ethics <https://neurips.cc/public/EthicsGuidelines>?

Answer: [Yes]

Justification: The research uses only publicly available datasets, complies with best practices for reproducibility, and does not raise ethical concerns.

Guidelines:

- If “No”, explain the special circumstances requiring deviation; preserve anonymity as required.

10. Broader impacts

Question: Does the paper discuss both potential positive societal impacts and negative societal impacts of the work performed?

Answer: [NA]

Justification: This work proposes a training algorithm and does not directly deploy an application with societal impacts; we discuss potential implications where relevant.

Guidelines:

- If NA or No, explain why impacts are out of scope.
- If applicable, discuss misuse risks and possible mitigations.

11. Safeguards

Question: Does the paper describe safeguards that have been put in place for responsible release of data or models that have a high risk for misuse (e.g., pretrained language models, image generators, or scraped datasets)?

Answer: [NA]

Justification: The paper does not release high-risk assets; standard benchmarks and models are reused under permissible terms.

Guidelines:

- If releasing high-risk assets, describe safeguards (access controls, filters, usage guidelines).

12. Licenses for existing assets

Question: Are the creators or original owners of assets (e.g., code, data, models), used in the paper, properly credited and are the license and terms of use explicitly mentioned and properly respected?

Answer: [Yes]

Justification: All datasets (OpenWebText, Alpaca, TinyStories) and baselines (e.g., GPT-Neo, ZeRO) are cited with sources/authors and licenses where applicable (Sections 4.3, 4.4, and references).

Guidelines:

- Cite originals, state versions/URLs, and include license names (e.g., CC-BY 4.0).

13. New assets

Question: Are new assets introduced in the paper well documented and is the documentation provided alongside the assets?

Answer: [NA]

Justification: No new datasets or models are released in this work.

Guidelines:

- If releasing assets, include documentation, license, limitations, consent, and anonymization at submission time if needed.

14. Crowdsourcing and research with human subjects

Question: For crowdsourcing experiments and research with human subjects, does the paper include the full text of instructions given to participants and screenshots, if applicable, as well as details about compensation (if any)?

Answer: [NA]

Justification: This paper does not involve human subjects or crowdsourcing.

Guidelines:

- If central to the paper, include as much detail as possible in the main text; compensation should meet local minimum wage.

15. Institutional review board (IRB) approvals or equivalent for research with human subjects

Question: Does the paper describe potential risks incurred by study participants, whether such risks were disclosed to the subjects, and whether IRB approvals (or equivalent) were obtained?

Answer: [NA]

Justification: No human subjects are involved.

Guidelines:

- If obtained, clearly state IRB (or equivalent) approval; keep anonymity for initial submissions.

16. Declaration of LLM usage

Question: Does the paper describe the usage of LLMs if it is an important, original, or non-standard component of the core methods in this research?

Answer: [Yes]

Justification: The paper centers on LLM training/fine-tuning; usage appears throughout (e.g., GPT-Neo 125M/2.7B in Sections 4.4, 4.5).

Guidelines:

- See LLM policy: <https://neurips.cc/Conferences/2025/LLM>.

A Experimental Details and Further Results

A.1 Pre-training on TinyStories

For experiments in Sec. 4.3, we used the configuration available on the Huggingface Hub ¹. We trained our own 10k vocabulary tokenizer on the dataset. We also report in Fig. 10 the results of our study on the impact of halving the batch size for DPU by not performing any gradient accumulation (*i.e.*, performing an optimizer’s step at each communication).

¹Tiny Stories Available at: <https://huggingface.co/datasets/roneneldan/TinyStories>

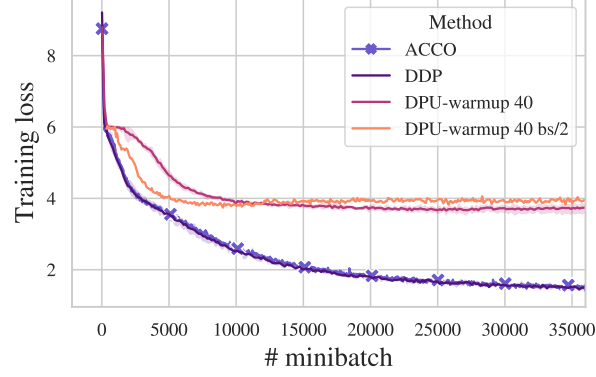


Figure 10: Comparison between running DPU on 8 GPUs with 2 steps of gradient accumulation on each (to match the standard batch-size) and DPU with only 1 gradient accumulation step. Doing so allows to double the number of optimizer’s step per minibatch, but divides the effective batch size by 2. This leads to faster convergence early in the training, but worse training loss in the end.

A.2 Proofs of Sec. 3

We first prove the convergence of ACCO in the Gradient Descent case.

Proposition A.1 (Gradient Descent Case). *Let $f : \mathbb{R}^d \rightarrow \mathbb{R}$ be an L -smooth function, and consider the iterates defined by*

$$\theta_{t+1} = \theta_t - \frac{\eta}{2} \left(\nabla f(\theta_t) + \nabla f(\tilde{\theta}_t) \right), \quad \tilde{\theta}_{t+1} = \theta_t - \eta \nabla f(\tilde{\theta}_t),$$

initialized at $\theta_0, \tilde{\theta}_0 \in \mathbb{R}^d$. Assume that f admits a global minimizer $\theta^ \in \arg \min f$. Then, for any $T > 0$ and step size $\eta \leq \frac{1}{L}$, the following bound holds:*

$$\frac{1}{T} \sum_{t=0}^{T-1} \left(\|\nabla f(\theta_t)\|^2 + \|\nabla f(\tilde{\theta}_t)\|^2 \right) \leq \frac{8}{\eta T} \left(f(\theta_0) + f(\tilde{\theta}_0) - 2f(\theta^*) + L\|\theta_0 - \tilde{\theta}_0\|^2 \right).$$

Proof. We define the Lyapunov potential:

$$V(\theta, \tilde{\theta}) := (f(\theta) - f(\theta^*)) + \eta L \left(f(\tilde{\theta}) - f(\theta^*) \right) + L\|\theta - \tilde{\theta}\|^2.$$

Using the L -smoothness of f , we apply the standard descent lemma:

$$\begin{aligned}
f(\theta_{t+1}) - f(\theta_t) &\leq -\frac{\eta}{2} \nabla f(\theta_t)^\top \left(\nabla f(\theta_t) + \nabla f(\tilde{\theta}_t) \right) + \frac{L\eta^2}{8} \left\| \nabla f(\theta_t) + \nabla f(\tilde{\theta}_t) \right\|^2 \\
&= -\frac{\eta}{2} \left\| \nabla f(\theta_t) \right\|^2 - \frac{\eta}{2} \langle \nabla f(\theta_t), \nabla f(\tilde{\theta}_t) \rangle \\
&\quad + \frac{L\eta^2}{8} \left(\left\| \nabla f(\theta_t) \right\|^2 + \left\| \nabla f(\tilde{\theta}_t) \right\|^2 + 2 \langle \nabla f(\theta_t), \nabla f(\tilde{\theta}_t) \rangle \right) \\
&= \left(-\frac{\eta}{2} + \frac{L\eta^2}{8} \right) \left\| \nabla f(\theta_t) \right\|^2 + \frac{L\eta^2}{8} \left\| \nabla f(\tilde{\theta}_t) \right\|^2 + \left(-\frac{\eta}{2} + \frac{L\eta^2}{4} \right) \langle \nabla f(\theta_t), \nabla f(\tilde{\theta}_t) \rangle \\
&= \left(-\frac{\eta}{2} + \frac{L\eta^2}{8} \right) \left\| \nabla f(\theta_t) \right\|^2 + \frac{L\eta^2}{8} \left\| \nabla f(\tilde{\theta}_t) \right\|^2 \\
&\quad + \left(-\frac{\eta}{2} + \frac{L\eta^2}{4} \right) \cdot \frac{1}{2} \left(\left\| \nabla f(\theta_t) \right\|^2 + \left\| \nabla f(\tilde{\theta}_t) \right\|^2 - \left\| \nabla f(\theta_t) - \nabla f(\tilde{\theta}_t) \right\|^2 \right) \\
&= \left(-\frac{\eta}{2} + \frac{L\eta^2}{8} + \frac{1}{2} \left(-\frac{\eta}{2} + \frac{L\eta^2}{4} \right) \right) \left\| \nabla f(\theta_t) \right\|^2 \\
&\quad + \left(\frac{L\eta^2}{8} + \frac{1}{2} \left(-\frac{\eta}{2} + \frac{L\eta^2}{4} \right) \right) \left\| \nabla f(\tilde{\theta}_t) \right\|^2 \\
&\quad - \frac{1}{2} \left(-\frac{\eta}{2} + \frac{L\eta^2}{4} \right) \left\| \nabla f(\theta_t) - \nabla f(\tilde{\theta}_t) \right\|^2 \\
&= \left(-\frac{3\eta}{4} + \frac{L\eta^2}{4} \right) \left\| \nabla f(\theta_t) \right\|^2 + \left(-\frac{\eta}{4} + \frac{L\eta^2}{4} \right) \left\| \nabla f(\tilde{\theta}_t) \right\|^2 \\
&\quad + \left(\frac{\eta}{4} - \frac{L\eta^2}{8} \right) \left\| \nabla f(\theta_t) - \nabla f(\tilde{\theta}_t) \right\|^2 \\
&\leq \left(-\frac{3\eta}{4} + \frac{L\eta^2}{4} \right) \left\| \nabla f(\theta_t) \right\|^2 + \left(-\frac{\eta}{4} + \frac{L\eta^2}{4} \right) \left\| \nabla f(\tilde{\theta}_t) \right\|^2 \\
&\quad + \left(\frac{\eta}{4} - \frac{L\eta^2}{8} \right) L^2 \left\| \theta_t - \tilde{\theta}_t \right\|^2
\end{aligned}$$

For the second point update, again using smoothness:

$$\begin{aligned}
f(\tilde{\theta}_{t+1}) - f(\tilde{\theta}_t) &\leq \nabla f(\tilde{\theta}_t)^\top \left(\theta_t - \tilde{\theta}_t - \eta \nabla f(\tilde{\theta}_t) \right) + \frac{L}{2} \left\| \theta_t - \tilde{\theta}_t - \eta \nabla f(\tilde{\theta}_t) \right\|^2 \\
&= \frac{1}{2\eta} \left\| \theta_t - \tilde{\theta}_t \right\|^2 + \left(\frac{\eta}{2} - \eta \right) \left\| \nabla f(\tilde{\theta}_t) \right\|^2 + \left(\frac{L}{2} - \frac{1}{2\eta} \right) \left\| \theta_t - \tilde{\theta}_t - \eta \nabla f(\tilde{\theta}_t) \right\|^2 \\
&= \frac{1}{2\eta} \left\| \theta_t - \tilde{\theta}_t \right\|^2 + -\frac{\eta}{2} \left\| \nabla f(\tilde{\theta}_t) \right\|^2 + \left(\frac{L}{2} - \frac{1}{2\eta} \right) \left\| \theta_t - \tilde{\theta}_t - \eta \nabla f(\tilde{\theta}_t) \right\|^2
\end{aligned}$$

The change in the regularization term satisfies, using L -smoothness:

$$\left\| \theta_{t+1} - \tilde{\theta}_{t+1} \right\|^2 - \left\| \theta_t - \tilde{\theta}_t \right\|^2 = \frac{\eta^2}{4} \left\| \nabla f(\theta_t) - \nabla f(\tilde{\theta}_t) \right\|^2 - \left\| \theta_t - \tilde{\theta}_t \right\|^2 \leq \left(\frac{L^2\eta^2}{4} - 1 \right) \left\| \theta_t - \tilde{\theta}_t \right\|^2.$$

Thus, for the sake of readability if $0 \leq \eta \leq \frac{1}{2L}$, we have that:

$$f(\theta_{t+1}) - f(\theta_t) \leq -\frac{1}{8}\eta \left\| \nabla f(\theta_t) \right\|^2 - \frac{1}{8}\eta \left\| \nabla f(\tilde{\theta}_t) \right\|^2 + \frac{L}{8} \left\| \theta_t - \tilde{\theta}_t \right\|^2 \quad (1)$$

and

$$f(\tilde{\theta}_{t+1}) - f(\tilde{\theta}_t) \leq \frac{1}{2\eta} \|\theta_t - \tilde{\theta}_t\|^2$$

and

$$\|\theta_{t+1} - \tilde{\theta}_{t+1}\|^2 - \|\theta_t - \tilde{\theta}_t\|^2 \leq -\frac{3}{4} \|\theta_t - \tilde{\theta}_t\|^2$$

Combining the three terms (two function values and one regularizer), the total Lyapunov change is:

$$\begin{aligned} V(\theta_{t+1}, \tilde{\theta}_{t+1}) - V(\theta_t, \tilde{\theta}_t) &\leq -\frac{1}{8}\eta \|\nabla f(\theta_t)\|^2 - \frac{1}{8}\eta \|\nabla f(\tilde{\theta}_t)\|^2 + \left(\frac{L}{8} + \frac{L}{2} - \frac{3L}{4}\right) \|\theta_t - \tilde{\theta}_t\|^2 \\ &\leq -\frac{1}{8}\eta \|\nabla f(\theta_t)\|^2 - \frac{1}{8}\eta \|\nabla f(\tilde{\theta}_t)\|^2 \end{aligned}$$

Summing over $t = 0$ to $T - 1$ and noting $V(\theta_T, \tilde{\theta}_T) \geq 0$, we conclude:

$$\sum_{t=0}^{T-1} \left(\|\nabla f(\theta_t)\|^2 + \|\nabla f(\tilde{\theta}_t)\|^2 \right) \leq \frac{4}{\eta} (V(\theta_0, \tilde{\theta}_0) - V(\theta_T, \tilde{\theta}_T)) \leq \frac{8}{\eta} \left(f(\theta_0) + f(\tilde{\theta}_0) - 2f(\theta^*) + L\|\theta_0 - \tilde{\theta}_0\|^2 \right).$$

Dividing both sides by T gives the claimed result. \square

We now prove the convergence of ACCO in the Stochastic Gradient Descent case.

Proposition A.2 (Stochastic Gradient Descent Case with Bounded Variance). *Let $f : \mathbb{R}^d \rightarrow \mathbb{R}$ be an L -smooth function, and let $\theta_0 = \tilde{\theta}_0 \in \mathbb{R}^d$ be the initialization. Suppose we perform the updates:*

$$\theta_{t+1} = \theta_t - \frac{\eta}{2} (g_t + \tilde{g}_t), \quad \tilde{\theta}_{t+1} = \theta_t - \eta \tilde{g}_t,$$

where g_t and \tilde{g}_t are unbiased stochastic gradients of f , conditionally independent, at θ_t and $\tilde{\theta}_t$ respectively:

$$\mathbb{E}[g_t \mid \theta_t, \tilde{\theta}_t] = \nabla f(\theta_t), \quad \mathbb{E}[\tilde{g}_t \mid \theta_t, \tilde{\theta}_t] = \nabla f(\tilde{\theta}_t),$$

and assume the variance is bounded as

$$\mathbb{E}[\|g_t - \nabla f(\theta_t)\|^2] \leq \sigma^2, \quad \mathbb{E}[\|\tilde{g}_t - \nabla f(\tilde{\theta}_t)\|^2] \leq \sigma^2.$$

Then, for any $T > 0$ and step size $\eta \leq \frac{1}{2L}$, it holds that

$$\frac{1}{T} \sum_{t=0}^{T-1} \mathbb{E}[\|\nabla f(\theta_t)\|^2 + \|\nabla f(\tilde{\theta}_t)\|^2] \leq \frac{16}{\eta T} (f(\theta_0) - f(\theta^*)) + 8\sigma^2 L\eta.$$

Proof. Using the same approach as in the full gradient case and L -smoothness, we get:

$$\begin{aligned} \mathbb{E}[f(\theta_{t+1}) \mid \theta_t, \tilde{\theta}_t] &\leq f(\theta_t) - \frac{\eta}{2} \nabla f(\theta_t)^\top \mathbb{E}[g_t + \tilde{g}_t \mid \theta_t, \tilde{\theta}_t] + \frac{L\eta^2}{8} \mathbb{E}[\|g_t + \tilde{g}_t\|^2 \mid \theta_t, \tilde{\theta}_t], \\ \mathbb{E}[f(\tilde{\theta}_{t+1}) \mid \theta_t, \tilde{\theta}_t] &\leq f(\tilde{\theta}_t) + \nabla f(\tilde{\theta}_t)^\top (\theta_t - \tilde{\theta}_t - \eta \mathbb{E}[\tilde{g}_t \mid \theta_t, \tilde{\theta}_t]) + \frac{L}{2} \mathbb{E}[\|\theta_t - \tilde{\theta}_t - \eta \tilde{g}_t\|^2 \mid \theta_t, \tilde{\theta}_t]. \end{aligned}$$

We also expand the expected change in the quadratic term:

$$\begin{aligned} \mathbb{E}[\|\theta_{t+1} - \tilde{\theta}_{t+1}\|^2 \mid \theta_t, \tilde{\theta}_t] &= \mathbb{E}\left[\left\|\frac{\eta}{2}(g_t - \tilde{g}_t) + (\theta_t - \tilde{\theta}_t)\right\|^2 \mid \theta_t, \tilde{\theta}_t\right] \\ &= \|\theta_t - \tilde{\theta}_t\|^2 + \frac{\eta^2}{4} \mathbb{E}[\|g_t - \tilde{g}_t\|^2 \mid \theta_t, \tilde{\theta}_t] + \eta \langle \theta_t - \tilde{\theta}_t, \mathbb{E}[g_t - \tilde{g}_t \mid \theta_t, \tilde{\theta}_t] \rangle. \end{aligned}$$

Further simplifications give

$$\mathbb{E} \left[\|\theta_t - \tilde{\theta}_t - \eta \tilde{g}_t\|^2 \mid \theta_t, \tilde{\theta}_t \right] = \|\theta_t - \tilde{\theta}_t - \eta \nabla f(\tilde{\theta}_t)\|^2 + \eta^2 \text{Var}(\tilde{g}_t \mid \tilde{\theta}_t),$$

$$\mathbb{E} \left[\|g_t + \tilde{g}_t\|^2 \mid \theta_t, \tilde{\theta}_t \right] = \|\nabla f(\theta_t) + \nabla f(\tilde{\theta}_t)\|^2 + \text{Var}(g_t \mid \theta_t) + \text{Var}(\tilde{g}_t \mid \tilde{\theta}_t),$$

$$\mathbb{E} \left[\|g_t - \tilde{g}_t\|^2 \mid \theta_t, \tilde{\theta}_t \right] = \|\nabla f(\theta_t) - \nabla f(\tilde{\theta}_t)\|^2 + \text{Var}(g_t \mid \theta_t) + \text{Var}(\tilde{g}_t \mid \tilde{\theta}_t).$$

Using the bounded variance a we can follow the same derivation as in the full-gradient case, with extra σ^2 terms appearing.

This yields:

$$\begin{aligned} \mathbb{E} \left[V(\theta_{t+1}, \tilde{\theta}_{t+1}) \mid \theta_t, \tilde{\theta}_t \right] - V(\theta_t, \tilde{\theta}_t) &\leq -\frac{1}{8}\eta \|\nabla f(\theta_t)\|^2 - \frac{1}{8}\eta \|\nabla f(\tilde{\theta}_t)\|^2 \\ &\quad + \sigma^2 \left(\frac{L\eta^2}{4} + \frac{L^2\eta^3}{2} + \frac{L\eta^2}{4} \right). \end{aligned}$$

Taking expectations and summing over $t = 0$ to $T - 1$, then rearranging and using $0 \leq \eta T \leq \frac{1}{2}$ and $\theta_0 = \tilde{\theta}_0$, we obtain:

$$\frac{1}{T} \sum_{t=0}^{T-1} \mathbb{E} \left[\|\nabla f(\theta_t)\|^2 + \|\nabla f(\tilde{\theta}_t)\|^2 \right] \leq \frac{16}{\eta T} (f(\theta_0) - f(\theta^*)) + 8\sigma^2 L\eta.$$

□

Note that it would be possible to derive bounds for non-increasing step size, as $V(\theta, \tilde{\theta}, \eta) := (f(\theta) - f(\theta^*)) + \eta L (f(\tilde{\theta}) - f(\theta^*)) + L\|\theta - \tilde{\theta}\|^2$ satisfies $V(\theta, \tilde{\theta}, \eta) \leq V(\theta, \tilde{\theta}, \tilde{\eta})$ for $\eta \leq \tilde{\eta}$.

A.3 Pre-training on OpenWebText

For all pre-training experiments on OpenWebText, the configuration used to instantiate the GPTNeo 125M is available on the Huggingface Hub². We only changed the "max_position_embeddings" parameter from 2048 to 1024. More details are displayed in Tab. 4. We used the OpenWebText dataset available on Huggingface³. We also report in Fig. 11 further results for the pre-training on H100 GPUs.

A.4 Instruction Fine-Tuning

For all fine-tuning experiments, we used the pre-trained GPT-neo 2.7B available on the Huggingface Hub⁴ and the associated tokenizer. We used the Alpaca dataset available on Huggingface⁵. More details are displayed in Tab. 5. We also report in Fig. 12 further results on the experiment described in Sec. 4.5.

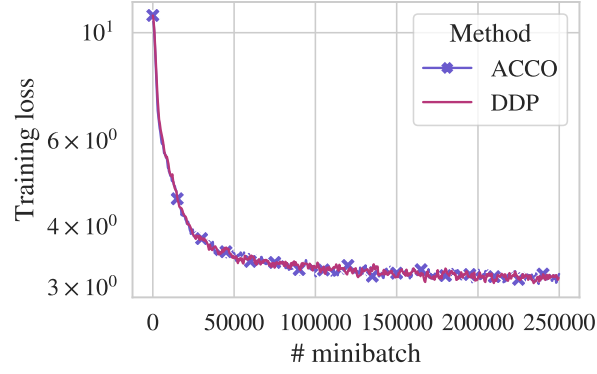


Figure 11: Training loss during training on OpenWebText with 8 H100 GPUs and 6B tokens.

Table 4: Training hyperparameters for ACCO and DDP configurations.

| Hyperparameter | 8 H100 | 32 A100 |
|---------------------|---------------|---------------|
| mini-batch_size | 24 | 24 |
| n_grad_accumulation | ACCO: -DDP: 1 | ACCO: -DDP: 1 |
| sequence_len | 1024 | 1024 |
| #tokens_batch | 400K | 1.5M |
| optimizer | AdamW | AdamW |
| learning_rate | 6e-4 | 6e-4 |
| weight_decay | 0.1 | 0.1 |
| adam_beta1 | 0.9 | 0.9 |
| adam_beta2 | 0.95 | 0.95 |
| nb_steps_tot | 50000 | 50000 |
| scheduler | cosine | cosine |
| n_warmup_steps | 0 | 0 |

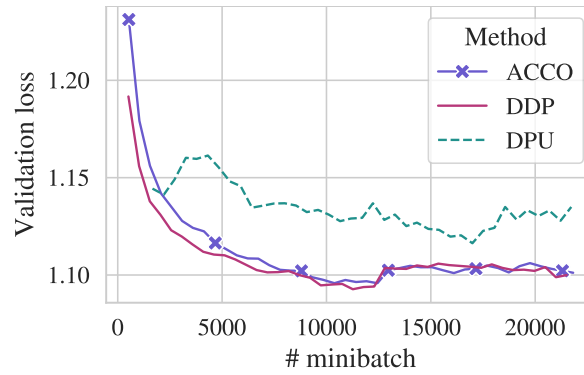


Figure 12: Validation curve with 8 workers on a single node.



Figure 13: Nsight system profile of our implementation of ACCO: our two streams do run in parallel. In this Figure, the computation take more time than the communication because we only profiled small scale experiments with 8 workers, and small number of parameters (36M as we profiled on our TinyStories [16] setting). This changes when using larger models and more workers, as seen in 4.1.

Table 5: Finetuning hyperparameters for ACCO, DDP and DPU configurations.

| Hyperparameter | ACCO | DDP | DPU |
|---------------------|--------|--------|--------|
| mini-batch_size | 4 | 4 | 4 |
| n_grad_accumulation | 2 | 4 | 4 |
| total batch_size | 128 | 128 | 128 |
| optimizer | AdamW | AdamW | AdamW |
| learning_rate | 2e-5 | 2e-5 | 2e-5 |
| weight_decay | 0.0 | 0.0 | 0.0 |
| adam_beta1 | 0.9 | 0.9 | 0.9 |
| adam_beta2 | 0.95 | 0.95 | 0.95 |
| nb_steps_tot | 50000 | 50000 | 50000 |
| scheduler | cosine | cosine | cosine |
| n_warmup_steps | 0 | 0 | 50 |

B Implementation Details

B.1 Profiling Results

B.2 Algorithm Pseudo-Code

We present our algorithm for time-varying batch size $N_i^{(t)}$.

²GPT-neo 125M Configuration Available at: <https://huggingface.co/EleutherAI/gpt-neo-125m/blob/main/config.json>

³OpenWebText Dataset Available at: <https://huggingface.co/datasets/Skylion007/openwebtext>

⁴GPT-neo 2.7B Available at: <https://huggingface.co/EleutherAI/gpt-neo-2.7B>

⁵Alpaca Dataset Available at: <https://huggingface.co/datasets/tatsu-lab/alpaca>

B.3 Slurm script to reproduce our results

Listing 1: SLURM and ACCO fine-tuning configuration

```
#SBATCH --nodes=2 # Request 2 nodes
#SBATCH --gres=gpu:1 # 1 GPU per node
#SBATCH --ntasks-per-node=1 # 1 task per node

acco-ft:
  group_by_length: false
  batch_size: 4
  n_grad_accumulation: 4
  learning_rate: 1e-5
  weight_decay: 0.0
  adam_beta1: 0.9
  adam_beta2: 0.95
  nb_steps_tot: 50000
  dataloader_num_workers: 1
  dataloader_pin_memory: True
  dataloader_persistent_workers: True
  label_smoothing_factor: 0
  max_length: 512
  scheduler_name: 'cosine'
  warmup: 0
  save: False
  use_mixed_precision: True
  n_warmup_steps: 0
  run_baseline_ddp: False # True for DDP
  method_name: 'acco' # 'ddp' for DDP
  #gradient_accumulation_steps: 1 # Add for DDP
  eval: True
  eval_step: 10
  run_expe_slow: False
  const_len_batch: False
  finetune: True
```

Algorithm 1 Training with ACCO in parallel for a worker i

```

1: Input: Model with differentiable loss  $F$ , number of models  $N$ , initial parameters  $\theta^{(0)}$ , training
   steps  $T$ , dataset shards  $\mathcal{D}_i$ .
2: Initialize: gradients  $g_i^{(-1)} = \nabla F(\theta^{(0)}, \xi_i^{(0)})$  and number of gradients  $N_i^{(-1)} = 1$ 
3: # Computation stream
4: while  $t < T$  do
5:   Stage 1.
6:   while not Ready_for_Stage_2 do
7:      $\xi_i^{(t)} \leftarrow \mathcal{D}_i$ 
8:      $g_i^{(t)} \leftarrow g_i^{(t-1)} + \nabla F(\theta^{(t)}, \xi_i^{(t)})$ 
9:      $N_i^{(t)} \leftarrow N_i^{(t-1)} + 1$ 
10:     $\tilde{\theta}^{(t+1)} \leftarrow \text{Buffer}_i$ 
11:     $\text{Buffer}_i \leftarrow (N_i^{(t)}, g_i^{(t)})$ 
12:   Stage 2.
13:   while not Ready_for_Stage_1 do
14:      $\xi_i^{(t)} \leftarrow \mathcal{D}_i$ 
15:      $\tilde{g}_i^{(t)} \leftarrow \tilde{g}_i^{(t-1)} + \nabla F(\tilde{\theta}^{(t+1)}, \xi_i^{(t)})$ 
16:      $\tilde{N}_i^{(t)} \leftarrow \tilde{N}_i^{(t-1)} + 1$ 
17:      $t \leftarrow t + 1$ 
18:      $\theta^{(t+1)} \leftarrow \text{Buffer}_i$ 
19:      $\text{Buffer}_i \leftarrow (\tilde{N}_i^{(t)}, \tilde{g}_i^{(t)})$ 
20:
21: # Communication stream
22: while True do
23:   Stage 1.
24:    $(\tilde{N}_i^{(t)}, \tilde{g}_i^{(t)}) \leftarrow \text{Buffer}_i$ 
25:    $\sum_i \tilde{N}_i^{(t)} \leftarrow \text{All\_Reduce}(\tilde{N}_i^{(t)})$ 
26:    $\text{Shard}_i \left( \sum_i g_i^{(t)} \right) \leftarrow \text{Reduce\_Scatter}(\tilde{g}_i^{(t)})$ 
27:    $\text{Shard}_i \left( \tilde{\theta}^{(t+1)} \right) \leftarrow \text{ShardedOpt} \left( \text{Shard}_i \left( \theta^{(t)} \right), \text{Shard}_i \left( \frac{\sum_i \tilde{g}_i^{(t)}}{\sum_i \tilde{N}_i^{(t)}} \right) \right)$ 
28:    $\text{Buffer}_i \leftarrow \text{All\_Gather}(\text{Shard}_i \left( \tilde{\theta}^{(t+1)} \right))$ 
29:    $N_i^{(t)} \leftarrow 0$ 
30:   Ready_for_Stage_2  $\leftarrow$  True
31:   Ready_for_Stage_1  $\leftarrow$  False
32:   Stage 2.
33:    $(N_i^{(t)}, g_i^{(t)}) \leftarrow \text{Buffer}_i$ 
34:    $\sum_i N_i^{(t)} + \tilde{N}_i^{(t)} \leftarrow \text{All\_Reduce}(N_i^{(t)} + \sum_i \tilde{N}_i^{(t)})$ 
35:    $\text{Shard}_i \left( \sum_i g_i^{(t)} + \tilde{g}_i^{(t)} \right) \leftarrow \text{Reduce\_Scatter}(g_i^{(t)} + \sum_i \tilde{g}_i^{(t)})$ 
36:    $\text{Shard}_i \left( \theta^{(t+1)} \right) \leftarrow \text{ShardedOpt} \left( \text{Shard}_i \left( \theta^{(t)} \right), \text{Shard}_i \left( \frac{\sum_i g_i^{(t)} + \tilde{g}_i^{(t)}}{\sum_i N_i^{(t)} + \tilde{N}_i^{(t)}} \right) \right)$ 
37:    $\text{Buffer}_i \leftarrow \text{All\_Gather}(\text{Shard}_i \left( \theta^{(t+1)} \right))$ 
38:    $\tilde{N}_i^{(t)} \leftarrow 0$ 
39:   Ready_for_Stage_1  $\leftarrow$  True
40:   Ready_for_Stage_2  $\leftarrow$  False

```
